

Chapter 2

Oxidative Stress and Apoptosis Induced by Agrochemicals on ICG Cell Line

2.1 Introduction:

Pesticides are a diverse collection of chemicals that are often regarded as one of the major contributors to today's world's environmental pollution. More than 1000 active chemicals are sold as insecticides, herbicides, and fungicides, and these substances are among them. Over 98% of sprayed insecticides and 95% of applied herbicides reach a destination other than their targeted species, including air, water, bottom sediments, food and non-target living systems, including humans. Non-target species are harmed by these hazardous compounds, which are intended to kill pests. Endocrine disruptors include pesticides, which are a very diverse class of chemicals. The scientific community has recently focused on the critical need to understand the basic mechanisms of action and physiological effects of various pesticides (Marino et al., 2012).

Pesticides interfere with numerous control points in the signaling pathways when they are present in the body. As a result, the response cascade is either inhibited or amplified at the improper time and in the improper tissue (Swedenborg et al., 2009). Furthermore, there is sufficient evidence to suggest that certain pesticide and endocrine disruptor impacts on developmentally critical genes and processes are epigenetic, leading to epigenetic transgenerational transmission which entails a number of signaling pathways and their associated receptors (Fowler et al., 2012). A number of studies have found that few pesticides that act as estrogen mimics act by these pathways, which work outside the nucleus (Tilghman et al., 2010). Cellular outcomes such as cell proliferation,

death, and maturation are all controlled by signaling molecules like kinases. Xenobiotics activate extracellular-signal-regulated kinases pathways, which operate as signal integrators for the cell's inputs, allowing the cell to make a final choice about its ultimate fate (cell division, differentiation, death, or malignant transformation (Ghosh & Ray, 2012; Farkhondeh et al., 2020).

Apoptosis, or programmed cell death, is a complicated and tightly controlled process that aids in the elimination of unwanted or damaged cells as well as a number of normal biological functions such as cell growth and differentiation, homeostasis, and ageing (Agalakova & Gusev, 2012). Nuclear chromatin condensation, DNA fragmentation, mitochondrial disintegration, cell shrinkage, membrane blebbing, and the development of apoptotic bodies are all morphological alterations associated with apoptosis. The biochemical features include a delicate regulation of intracellular signaling pathways via gene expression and/or protein activity. Pesticide-induced apoptosis is caused by a variety of molecular mechanisms, including G protein-dependent signalling, oxidative stress, ATP depletion, activation of cell surface death receptors, disruption of the outer mitochondria membrane, activation of caspases, alteration in the ratio of anti-apoptotic-apoptotic Bcl-2 proteins, and upregulation of p53 expression, alteration in expression of apoptosis-related genes, endoplasmic reticulum stress and disturbances in protein synthesis. Cell to cell variations are an important determinant of cell fate, as to whether cells will survive or die by apoptosis following a toxic insult (Orrenius et al., 2011). These variations can result from differences in triggering signals and/or cellular state (e.g. genetic, phenotypic or stochastic fluctuations), cell cycle phase or cellular micro-environment (Flusberg & Sorger, 2015). It has been observed that pesticide exposure leads to a series of toxic effects, for example, it can increase superoxide radicals by attacking oxygen directly and interfering with oxygen metabolism, or

by attacking the system of antioxidant enzymes. Excessive superoxide radicals can cause lipid peroxidation of cell membrane and lead to eventually the dysfunction of the cells, gene mutation, protein crosslinking, and even cell death. During the period of oxidative damage, the antioxidants of comprehensive antioxidant systems in organism play important roles (Birben et al., 2012; Kurutas, 2016).

Fish cell lines are genuine non-animal alternatives in ecotoxicology (Halder et al., 2014; OECD, 2021). Several researchers investigated using cytotoxicity tests obtained from fish as an alternative to *In-vivo* experiments. Schirmer et al (2006) have advocated using fish cell lines in chemical and effluent testing. The rainbow trout (*Oncorhynchus mykiss*) cell line assay (RTgill-W1 cells) for predicting acute fish toxicity. In general, cell-based assays display lower sensitivity than *in vivo* techniques when comparing nominal effect concentrations (Lungu-Mitea et al., 2021). Reduced xenobiotic metabolism, decreased biological complexity, and decreased bioavailability of exposed chemicals all contribute to the differential in sensitivity (Groothuis et al., 2015). Furthermore, considering that fish and fish embryos are exposed to water, whereas cells are cultured in complicated cell culture medium, it might be owing to variations in experimental circumstances. Serum, protein, and lipids in the latter function as sinks for hydrophobic substances. As a result, the actual bioavailable concentration to the cells, the free concentration, is just a fraction of the total concentration, resulting in distinct interactions in both systems (Lungu-Mitea et al., 2021). In the first layer of genotoxicity testing for chemicals/pesticides, an *in vitro* test utilizing cells from homoeothermic species provides a potent alternative to using live animals (OECD, 2021). *In-vitro* tests provide a number of advantages, including cost, flexibility, waste volume, and the laboratory facilities required. As an alternative to acute fish bioassays, the established fish cell line derived from the

various tissue of fish, has been effectively utilized in cytotoxicity studies. Because it retains some capacity to metabolize xenobiotics without the requirement for an external metabolic system, this line gives highly valuable findings in cytotoxicity and investigations (Zurita et al., 2007).

In vitro cytotoxicity tests of organophosphates, carbamates and organochlorines have been studied, though not as extensively as the acute toxicity tests in fish. Various fish cell lines such as RTG-2 (fibroblasts from gonad tissue of rainbow trout (*Oncorhynchus mykiss*), GSF (fibroblasts from scale tissue of goldfish (*Carassius auratus*), R1 (fibroblasts from hepatic tissue of rainbow trout), FHM (fibroblast from fathead minnow (*Pimephales promelas*), CHSE-214 (epithelial cells from chinook salmon (*Oncorhynchus tshawytscha*) embryo), BF-2 (fibroblasts from truck of Bluegill (*Lepomis macrochirus*) fry and primary cell culture as rainbow trout gill epithelial cells and hepatocytes are applied to scan the cytotoxicity of this pesticides (Li & Zhang, 2001; Castaño & Gómez-Lechón, 2005; Chen et al., 2006; Marabini et al., 2011; Abdul Majeed et al., 2014; Lungu-Mitea et al., 2021).

Although we know little about the metabolism of many pesticide compounds, it is conceivable that they might be the cause of various aspects of the toxicity. Our previous *In vivo* studies on *Oreochromis mosambicus* and *Labeo rohita* have established the toxic potential of all AGs and have modulated and induced apoptosis (Patel, et al., 2016; Sadekarpawar, et al., 2010; Sadekarpawar, et al, 2015; Upadhyay, et al., 2016) After establishing the impact on the proliferation on ICG cell line on exposure of agrochemicals (Chapter I), our next target was:

1. To observe the morphological alterations in the cell line on exposure of AGs

2. To assess whether AGs have interfered with the antioxidant balance and resulted in generation of the reactive oxygen species (ROS), by quantifying the enzymatic and non-enzymatic antioxidant parameters.
3. To understand the altered mechanistic pathway leading to cell death qualitatively by AO/EB double staining and quantitatively by apoptotic markers and confirming with FACS

2.2 Materials and Methodology:

Cell Morphological Observation (Abdul Majeed et al., 2013): Cell morphological changes were observed using a light microscope. ICG cells (1.5×10^6 cells per well) were plated in 6 well plates (9.5cm^2 , TPC6, HiMedia, India). After 24 hr., cells were treated with different sub lethal concentration of agrochemicals like IMI, CZ, MN and PE for 7 days. Cell morphological characteristics, such as cell shrinkage or swelling, membrane blebbing, cytoplasmic vacuolization, and apoptotic body formation, were recorded using inverted light microscope.

H₂DCF-DA Staining: (Aranda et al., 2013; Choi et al., 2016)

Principle:

The 2', 7'-dichlorodihydrofluorescein diacetate (H₂DCF-DA/DCF-DA) fluorescent probe reacts with several ROS including hydrogen peroxide, hydrogen radicals and peroxynitrite. The cell-permanent lipophilic. H₂DCF-DA passively diffuses into cells and is retained in the intracellular level after cleavage by intracellular esterase. Upon Oxidation by ROS, the non-fluorescent H₂DCF-DA is converted to the highly fluorescent hydrophilic 2', 7'-dichlorofluorescence (DCF). The fluorescence intensity of DCF is proportional to the amount of ROS produced by the cells.

Method:

The production of intracellular ROS was measured by oxidation of DCF-DA. Prior to the use, H₂DCF-DA stock solution was prepared in DMSO (6644, SRL, India) under sterile condition in laminar flow hood and 1×10^5 cells were plated in the 6 well plate (9.5cm², TPC6, HiMedia, India). Cells were then treated with the sub lethal concentration – HD, MD, LD for all agrochemicals. After 7 days of treatment, the cells were washed twice with PBS (M1866, pH 7.4, HiMedia, India). Cells were then incubated with DCFH-DA dye (D399, Invitrogen™) at 37°C for 30 minutes to allow the diffusion of the fluorescent probe into the cells and its subsequent hydrolysis to non-fluorescence dichlorofluorescein (DCFH) under the action of intracellular esterase. Intracellular ROS generation was measured by fluorescence microscopy with the excitation and emission wavelengths set as 488 and 528 nm, respectively.

ROS Parameters:**Lipid Peroxidation (LPO) - Thiobarbituric Acid Reactive Species Assay (TBARS):**

The thiobarbituric acid reactive species (TBARS) level in cells was determined by the method of Ohkawa et al., (1979)

Principle:

This assay is based on the appearance of a red chromophore that absorbs at 532 nm following the reaction of Thiobarbituric acid (TBA) with malonyl dialdehyde (MDA) and other breakdown products of peroxidase lipids which together called as thiobarbituric acid reactive substances (TBARS).

Procedure:

To make 10% cell homogenate, cells were washed several times with 0.1 M phosphate buffered saline (PBS) (pH 7.4) and homogenized. Then, the tubes were prepared with mixture of solutions containing 0.2 ml of 8.1% sodium dodecyl sulphate (SDS), 1.5 ml of 20% acetic acid solution and 1.5 ml of 1% Thiobarbituric acid (TBA) solution in which 0.2 ml of 10% homogenate was added. The blank was prepared for each sample by replacing TBA solution with distilled water. The solution was mixed and heated in a water bath at 95 °C for 60 min. The tubes were then immediately cooled and 2 ml of aliquot was transferred to a centrifuge tube in which an equal volume of 10% TCA was added. The solution was mixed and centrifuged at 1000g for 15 minutes. The aliquot of the resulting supernatant fraction was read against blank on Systronics Digital Spectrophotometer at 532 nm.

$$\text{Concentration of MDA} = \frac{\text{O.D of sample} \times \text{dilution} \times 10^9}{\text{Control factor}(1.56 \times 10^5) \times 10^6 \text{cells}}$$

GSH (reduced glutathione)

The concentration of glutathione was assayed by the method of Ellman (1959).

Principle:

Glutathione (GSH) present in the cells oxidized 5, 5' – dithiobis-(2- nitrobenzoic acid), (DTNB) to form yellow coloured complex which can be read at 412 nm. The absorbance is proportional to amount of GSH.

Procedure:

Cells were homogenized in 3 ml phosphate buffer and precipitated with 2 ml of 10% TCA. Following to the centrifugation, 1 ml of supernatant was taken to

which 0.5 ml of Ellman's reagent (19.8 mg of 5, 5'- dithiobis-(2- nitrobenzoic acid) in 100 ml of 10% sodium citrate) and 3 ml of phosphate buffer was added. Blank was run without homogenate. Mixture was incubated at 37 °C for 30 min and absorbance was measured at 412 nm. GSH standards were treated in a similar way and the colour developed was read at 412 nm to make a linear plot. Absorbance of unknown samples were plotted against concentration with respect to standards. Glutathione levels were expressed as moles/ 2×10^6 cells.

Superoxide Dismutase (SOD) (Kakkar et al., 1984)**Principle:**

In this assay, the formazan formed at the end of reaction which indicates presence of the enzyme. One unit of the enzyme activity is defined as the enzyme concentration required to inhibit 50% of the optical density of chromogen formed in one minute at 560 nm under assay condition.

Procedure:

For the Superoxide dismutase assay, cells were washed with PBS in the tubes and then homogenized in cold normal saline which were subsequently centrifuged. The supernatant was discarded, 2 ml of 0.01% digitonin was added to the pellet to yield the enzyme extract. The tubes were incubated for 15 minutes, centrifuged at 3000 rpm and the supernatant was used as sample. In this procedure, control solution consists of 2.4 ml phosphate buffer (0.052 M sodium pyrophosphate buffer at a pH 8.4 adjusted with 0.052 M (Na H₂PO₄.H₂O), 0.1 ml of freshly prepared phenazine methosulphate (PMS; 186 µM in double distilled water). 0.3 ml of nitrate tetrazolium (NBT; 300 µM; freshly prepared in double distilled water) and 0.2 ml of enzyme was added prior to the addition of NADH in a total 3 ml of assay system. The reaction was stopped by the adding 1 ml of acetic acid

exactly 90 seconds after the addition of NADH. Then 4 ml of n- Butanol was added to the tubes and shaken vigorously to extract the formazon. Subsequently, the tubes were centrifuged for 10 minutes at 2000 rpm and supernatant was used for the measurement of optical density at 560 nm against butanol on a visible spectrophotometer.

Calculation: $\frac{\text{OD OF Control}}{\text{O.D of Sample}} \times \text{accuracy factor} \times \text{dilution} \div \text{STD Enzyme Unit}$

Where, accuracy factor = 1; dilution= 2.5; standard enzyme unit = 3.0

Enzyme activity = x/ mg protein

The activity was expressed as units SOD/ mg protein.

Catalase Activity:

The catalase activity was measured by the modified method of Sinha, (1972)

Procedure:

The incubation mixture had total volume of 2.0 ml, which contain 0.1 ml of dilute homogenate, 1.0 ml of phosphate buffer and 0.4 ml distilled water to which 0.5 ml of H₂O₂ solution was left out in control tubes. Then, it was incubated for 1 min at 37 °C and the reaction was stopped by the addition of 2.0 ml potassium dichromate acetic acid reagent. The samples were kept in boiling water bath for 15 minutes, finally cooled and then absorbance was measured at 570 nm against control.

Calculation:

$$\frac{\text{Absorbance of sample} \times \text{STD concentration}(\mu\text{mol})}{\text{Enzyme} \times \text{Std Absorbance} \times \text{protein} \left(\frac{\text{mg}}{\text{ml}}\right)}$$

AO/EB staining: (Ribble et al., 2005):

Acridine Orange (MB116, HiMedia) /Ethidium Bromide (MB071, HiMedia) staining is used to visualize nuclear changes and apoptotic body formation that are characteristic of apoptosis. Acridine Orange is a cell permeable nucleic acid selective dye that emits green fluorescence when bound to ssDNA or RNA (at 520 nm) and red fluorescence when bound to ssDNA or RNA(at 650 nm). Since it is a cationic dye, it also enters acidic compartments such as lysosomes which in low pH conditions, will emit orange light. The most commonly used stain for detecting DNA/RNA is ethidium bromide. Ethidium bromide is a DNA interchelator, inserting itself into the spaces between the base pairs of the double helix. Ethidium bromide possesses UV absorbance maximal at 300 and 360 nm. Additionally, it can absorb energy from nucleotides excited by absorbance of 260 nm radiation. Ethidium re-emits this energy as yellow/orange light centered at 590 nm.

Method:

The dual staining of acridine orange (MB116, HiMedia, India) and ethidium bromide (MB071, HiMedia, India) was used to measure live cells from apoptotic and necrotic cells(Liu et al., 2015). The cells were harvested and washed three times with PBS (M1866, pH 7.4, HiMedia, India) after being incubated with sub lethal concentration-LD, MD, HD of the all agrochemicals for 7days. Then the cells were stained with 100µl of AO and EB (to a final concentration of 100µg/ml for both) and incubated for 15 minutes at 37°C in dark and washed three times with PBS (M1866, pH 7.4, HiMedia, India). The morphology of the treated cells was examined by fluorescence microscopy.

Apoptosis Detection Assay (APOAF, Sigma-aldrich, USA)

Principle

Annexin V-FITC is a fluorescent probe which binds to phosphatidylserine in the presence of calcium. Apoptosis, or programmed cell death, is a mechanism of cells used to negatively select cells that are deleterious to the host. The cellular changes involved in the process include loss of phospholipid asymmetry during the early stages of apoptosis. In living cells, phosphatidylserine is transported to the inside of the lipid bilayer by the Mg-ATP dependent enzyme, aminophospholipid translocase. At the onset of apoptosis, phosphatidylserine, which is normally found on the internal part of the plasma membrane, becomes translocated to the external portion of the membrane. The phosphatidylserine becomes available to bind to the annexin V-FITC conjugate in the presence of calcium. The procedure consists of the binding of annexin V FITC to phosphatidylserine in the membrane of cells, which are beginning the apoptotic process, and the binding of propidium iodide to the cellular DNA in cells where the cell membrane has been totally compromised. The cells are incubated with annexin V-FITC and propidium iodide. After a 10 mins incubation period at room temperature the cells are analyzed by flow cytometry.

Method

The ICG cells treated with the LD, MD and HD of agrochemicals in 1×10^5 cells/ml cell concentration and were incubated for 7 days. The non-treated ICG cells at 1×10^5 cells/ml was considered as control. The cells were washed twice with PBS (M1866, pH 7.4, HiMedia, India). The cells were re-suspended in Binding Buffer at a concentration of 1×10^5 cells/ml and 500 μ l of the apoptotic cell suspension was added to a plastic 12 x 75 mm test tube. Further, 5 μ l of Annexin V FITC Conjugate and 10 μ l of Propidium Iodide solution was added to each cell suspension and was incubated at room temperature for 10 minutes in

darkness. The tubes were placed in the flow cytometer (FACS Calibur flow cytometer, Becton Dickinson, Singapore) and fluorescence was determined immediately. Three characteristic of cells were noted 1. Cells with an early apoptotic process- stained with Annexin V FITC Conjugate alone, 2. Live cells- with no staining by either Propidium Iodide solution or Annexin V FITC Conjugate and 3. Necrotic cells- stained with both Propidium Iodide Solution and Annexin V FITC Conjugate.

Total RNA Extraction (Trizol method)

Total RNA was extracted isolated from ICG cells from control and treated cells for all agrochemicals. 500 µl TRIzol reagent (15596-026, Invitrogen, USA) was added in each well and scraped out in 1.5 ml RNAse free tubes. For complete dissociation of nucleoprotein complexes, samples were incubated for 5 minutes at room temperature. The incubation was followed by the addition of chloroform (84155, SRL) and was vigorously shaken for effective mixing of both the solutions. The samples were kept at room temperature for 5 minutes till the aqueous and organic layers were distinct. Thereafter, the tubes were subjected to centrifugation at 12,000x g for 15 minutes at 4°C. The mixture got separated into a lower red phenol-chloroform phase, an interphase, and a colourless upper aqueous phase. An aliquot of upper aqueous phase was then transferred into a new 1.5 ml micro centrifuge tube. Precipitation was done by adding 500 µl of isopropanol (62986, SRL) to the supernatant that was transferred. The samples were kept in room temperature for 10 minutes, centrifuged at 12,000x G for 15 minutes at 4°C. After precipitation the supernatant was discarded without disturbing the pellet and was washed in 500 µl of 75% ethanol and then 500 µl absolute ethanol was added to the pellet. Effective mixing was done by gentle inversion and was further subjected to centrifugation at 7,500 x g for 5 minutes at 4°C. The pellet was re-suspended by adding 40 µl of DEPC (Diethylpyro

carbonate) water (DBOS009, SRL, India) was quantified spectrophotometrically using NanodropC and was stored in -20° C.

cDNA Synthesis

First strand of cDNA was synthesized from each sample using Thermo Scientific Verso cDNA Synthesis Kit (AB-1453/A). Verso Reverse Transcriptase Verso is an RNA-dependent DNA polymerase with a significantly attenuated RNase H activity. Verso can synthesize long cDNA strands, up to 11 kb, at a temperature range of 42 °C to 57 °C. In reaction, 1 µg RNA was used as a template for cDNA synthesis using oligo dT primers. The volume of each component is for a 20 µl final reaction. The Reaction mix is mentioned in Table given below.

	Volume
5X cDNA synthesis buffer	4 µl
dNTP Mix	2 µl
anchored oligo dT /random hexamers	1 µl
RT Enhancer	1 µl
Verso Enzyme Mix	1 µl
Template (RNA)	1- 5 µl
Molecular grade nuclease-free Water	To 20 µl
Total Volume	20 µl

Table 2. 1: Reaction mix for cDNA synthesis

Reverse transcription cycling program:

	Temperature	Time	Number of cycles
cDNA synthesis	42 °C	30 min	1 cycle
Inactivation	95 °C	2 min	1 cycle

Table 2. 2: Reverse transcription cycling program for cDNA synthesis

RT-PCR Amplification

Quantitative RT-PCR was performed using PowerUp SYBR Green Master Mix (A25741, Applied Biosystems, USA) in Quant Studio 12K (Life technology) FAST real-time PCR machine with primers to detect selected messenger RNA (mRNA) targets. The melting curve of each sample was measured to ensure the specificity of the products. GAPDH was used as an internal control to normalize the variability in the expression levels and data was analyzed using $2^{-\Delta\Delta CT}$ method (Livak and Schmittgen, 2001).

Component	Volume (20 μ L/well)
PowerUp SYBR Green Master Mix (2X)	10 μ l
Forward Primer (10uM)	1 μ l
Reverse Primer (10uM)	1 μ l
DNA Template	2 μ l
Molecular grade Nuclease free water	6 μ l
Total	20 μ l

Table 2. 3: Real Time PCR Reaction mix

Step	Temperature	Duration	Cycles
UDG activation	50°C	2 minutes	Hold
Dual- Lock DNA polymerase	95°C	2 minutes	Hold
Denature	95°C	3 seconds	40
Anneal/extend	60 °C	30 seconds	

Table 2.4 Real Time PCR condition

	Gene Name	Primer Type	Sequence	Tm
1	gapdh	Forward	CTCACACCAAGTGTCAGGACGAACAG	66.38
		Reverse	GTCAAGAAAGCAGCACGGGTCACC	66.13
1	bax	Forward	GGGAGCTGCACTTCTCAACAACCTTTG	64.8
		Reverse	ATTCATCTCCAGCATCCCGTAACAC	64.21
2	bcl2	Forward	TCCAAACTCTGACAGGAGGCTTCAGG	66.38
		Reverse	ATTCATCTCCAGCATCCCGTAACAC	63.22
3	caspase 3	Forward	GATGCCAAGCCTCAATCCCATG	62.12
		Reverse	GGTTCATGCCTGTCCTGCGATC	63.98
4	nfk b	Forward	GTACCTTGGAGGGAACTGGC	61.40
		Reverse	CATCCACAGGACCACCACTC	61.40
5	tnf α	Forward	CACACTGGGCTCTTCTTCGT	59.9
		Reverse	CAAACCTGACCTTACCCCGCT	59.9

Table 2.5 PCR real time PCR primer sequences

Statistical analysis

The computed data was analyzed using Graph Pad PRISM 9 software. One and two-way ANOVA followed by DUNNETs multiple comparison test were used to the test for significant differences among the individual treatment combinations. Statistical significance was accepted at $p < 0.05$ for all test.

2.3 Result:

In the present study light microscopic observation of the AG exposed cells discovered morphological alterations like altered cell shape, membrane blebbing, and detachment of cells as well as appearance of apoptotic bodies compared to the control cells which had intact cell morphology. Of all the AGs, the maximum

alterations were found with IMI and CZ in a dose dependent manner, whereas MN and PE exposure exhibited fewer alterations (Figure 3.1).

Figure 2.2 and 2.3 depicts the ROS generation tested by DCFH-DA staining. A significant ROS generation was observed in the treated cells compared to that of control. The order of emission was IMI>CZ>PE> MN indicating cytotoxic impact.

The results of enzymatic (SOD and Catalase) and non-enzymatic antioxidant activity (LPO and GSH) are represented in Figure 2.5 to 2.7 and Table 2.7. A significant dose dependent decline ($P<0.005$) was observed for SOD and Catalase levels. Maximum drop was established with IMI and CZ compared to control. As expected the non-enzymatic activity of LPO and GSH concurrently was found to show a significant ($P<0.005$) increase in LPO and decrease in GSH activity. The order of altered anti-oxidant status observed was: IMI>CZ>MN>PE.

In the present study AO/ EtBr double staining revealed a dose dependent apoptotic body formation with all the AGs. Maximum apoptotic bodies were observed in IMI treated cells and minimum apoptotic formation were seen on exposure of MN (Figure 2.9 and 2.10). The results of quantitative analysis of specific apoptotic markers (bax, caspase 3) clearly exhibited a significant dose dependent increase in their expression.

The order of altered expression was IMI>CZ>MN>PE. Whereas, the expression of anti-apoptotic markers (bcl2, nf κ b) were found to be decreasing (Figure 2.10 and 2.12) whereas the apoptotic markers like caspase and bax were found to be increase dose dependent manner. Percentage of cell death by FACS is represented in Figure 2.12 to 2.15) which depicts maximum cell death on exposure of IMI, where early and late apoptotic cells were found to be highest at high dose compared to control.

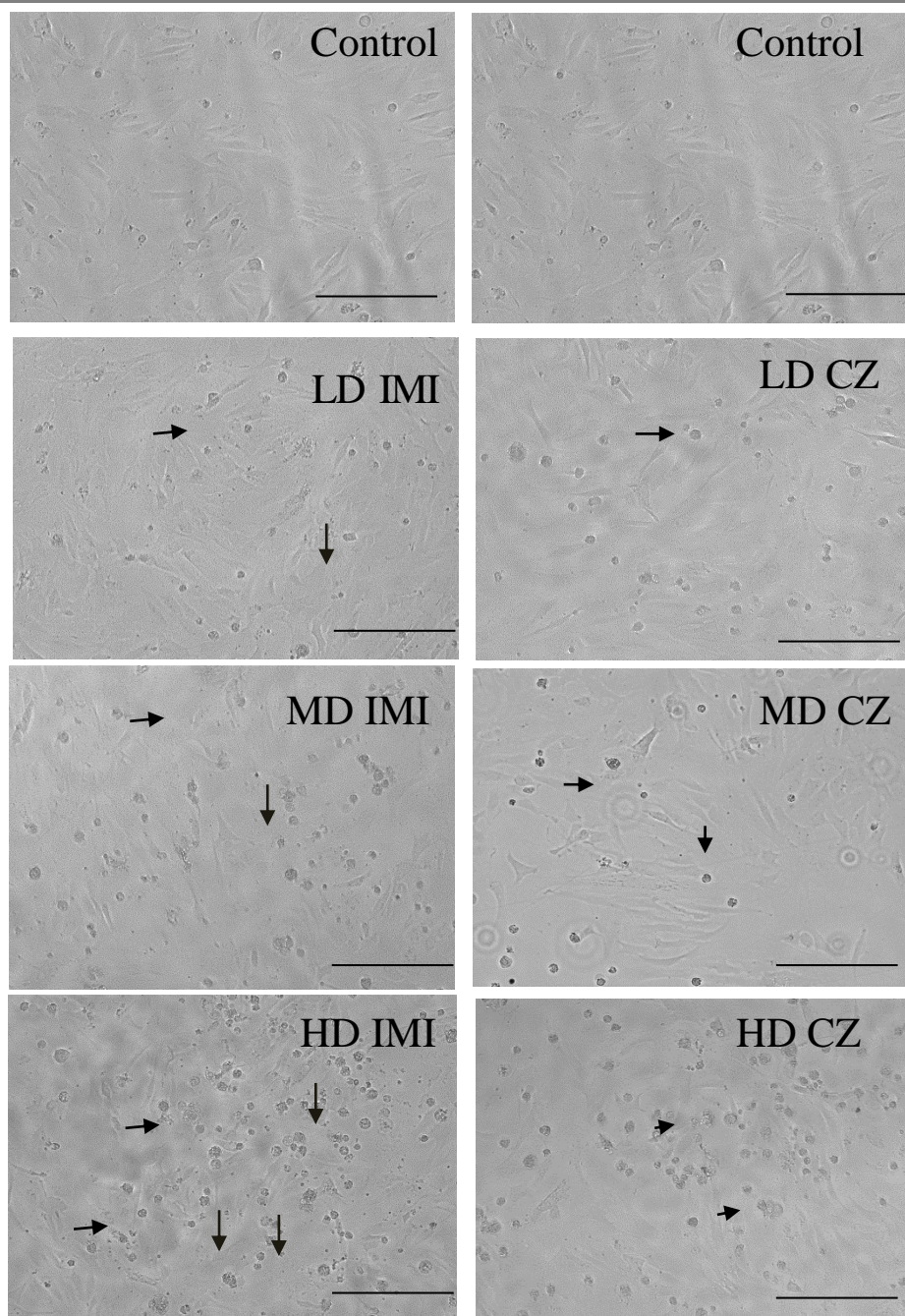


Figure 2.1a: Alteration in Cell Morphology of ICG Cells on Exposure of AGs

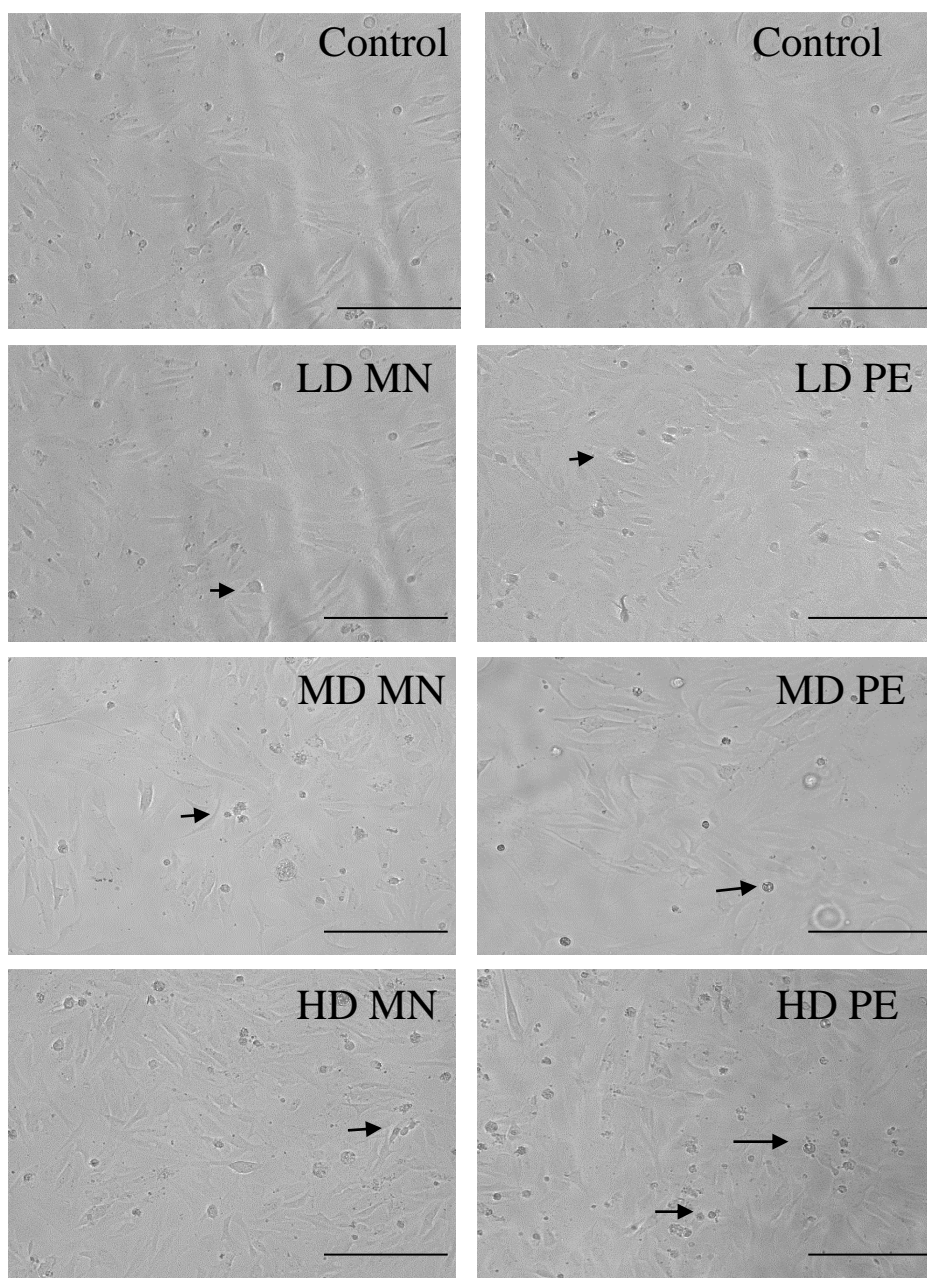


Figure 2.1b: Alteration in Cell Morphology of ICG Cells on Exposure of AGs

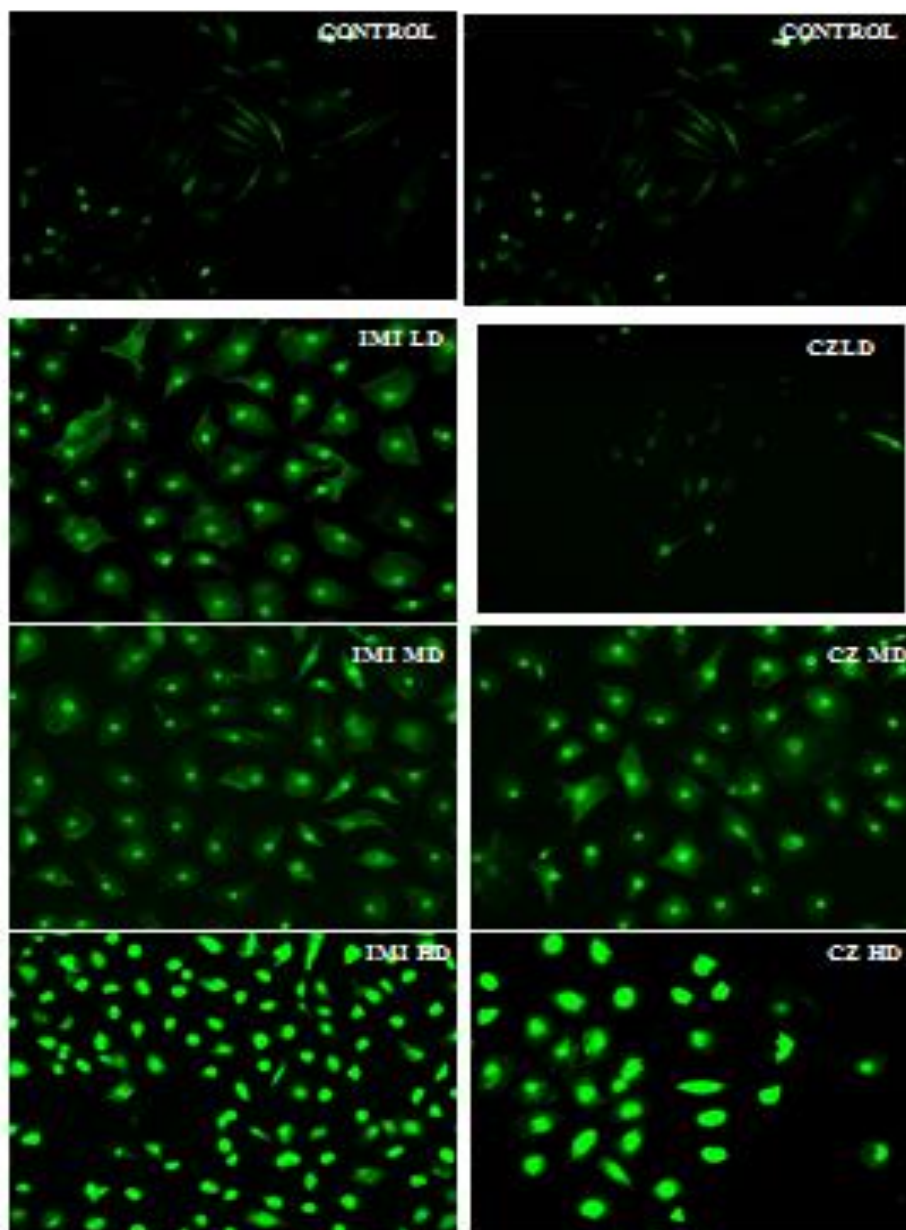


Figure 2.2 Results of DCF-DH staining for ROS Generation in ICG cell line after exposure of IMI and CZ with sub-lethal concentrations (LD, MD and HD).

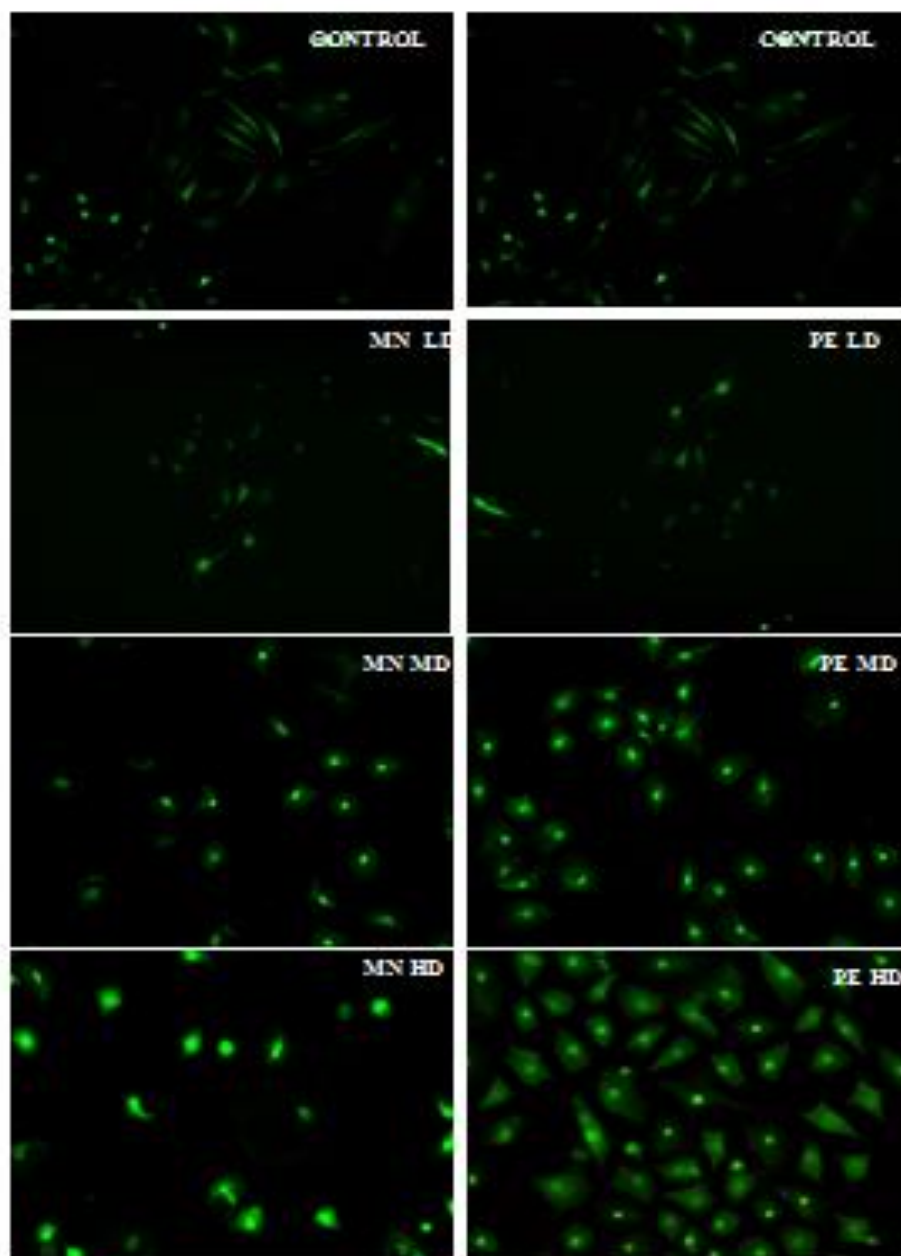


Figure 2.3 Results of DCF-DH staining for ROS Generation in ICG cell line after exposure of MN and PE with sub-lethal concentrations (LD, MD and HD)

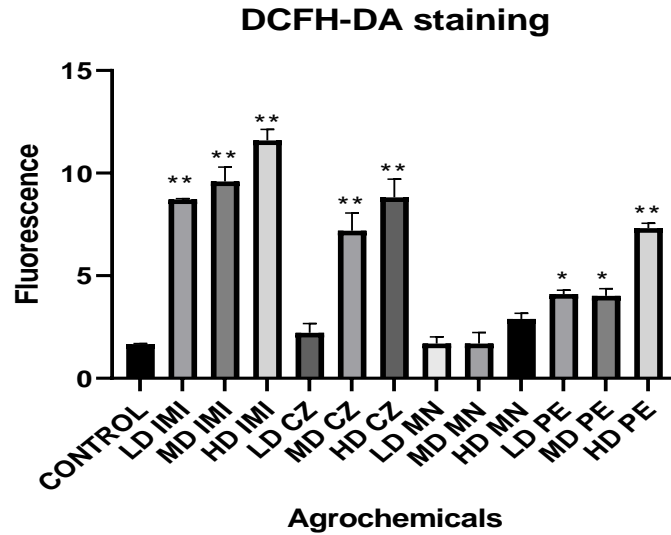


Figure 2.4 Depicts result of DCFDA staining in ICG cells exposed to AGs. Each value represents the mean ± SEM. (n=3), Significant level indicated by * $p < 0.05$; ** $p < 0.01$

Agrochemicals		Fluorescence
Control		1.666±0.023
IMI	LD	8.716±0.045**
	MD	9.593 ± 0.7**
	HD	11.59±0.54**
CZ	LD	2.219±0.45 ^{ns}
	MD	7.19±0.87**
	HD	8.813±0.89**
MN	LD	1.688 ± 0.33 ^{ns}
	MD	1.698±0.53 ^{ns}
	HD	2.897±0.27 ^{ns}
PE	LD	4.108±0.19*
	MD	4.0238±0.35*
	HD	7.322 ± 0.24**

Table 2.6 DCFDA fluorescence in ICG cells exposed to agrochemicals Each value represents the mean ± SEM. (n=3), Significant level indicated by * $p < 0.05$; ** $p < 0.01$

Agrochemicals	SOD	CAT	GSH	LPO
	$\mu\text{mol/mg}$ protein	$\mu\text{mol/mg}$ protein	$\mu\text{mol/mg}$ protein	$\mu\text{mol/mg}$ protein
Control	2.897±0.026	24.7±2.34	1.5±0.04	0.4±0.0032
LD IMI	2.46±0.045**	14.7±1.26*	1.02±0.05**	0.8±0.001
MD IMI	2.236±0.034**	9.76±1.76**	0.8±0.06**	1.02±0.06*
HD IMI	1.243±0.0035**	6.85±0.98***	0.3±0.003**	1.4±0.008**
LD CZ	2.6±0.002**	20.4±2.12	1.3±0.0023**	0.45±0.03
MD CZ	2.134±0.0025**	15.2±2.98	1±0.0043**	0.8±0.0034
HD CZ	1.432±0.0034**	11.8±1.54	0.7±0.003**	1.2±0.003**
LD MN	2.806±0.0012**	21.4±2.87	1.4±0.34**	0.5±0.34
MD MN	1.706±0.0014**	18.6±1.43	1.2±0.23**	0.7±0.23
HD MN	1.566±0.0026**	14.7±4.01*	0.9±0.006**	1.01±0.03*
LD PE	2.406±0.0032**	23.7±2.07	1.3±0.0013**	0.6±0.12
MD PE	1.587±0.0012**	19.5±2.16	1±0.003**	0.9±0.056
HD PE	1.678±0.002**	17.5±3.21**	0.5±0.0014**	1.1±0.0043**

Table 2.7 depicts the mean ± SEM. (n=3) values for SOD, CATALASE, GSH, LPO. Significant level indicated by * $p < 0.05$; ** $p < 0.01$

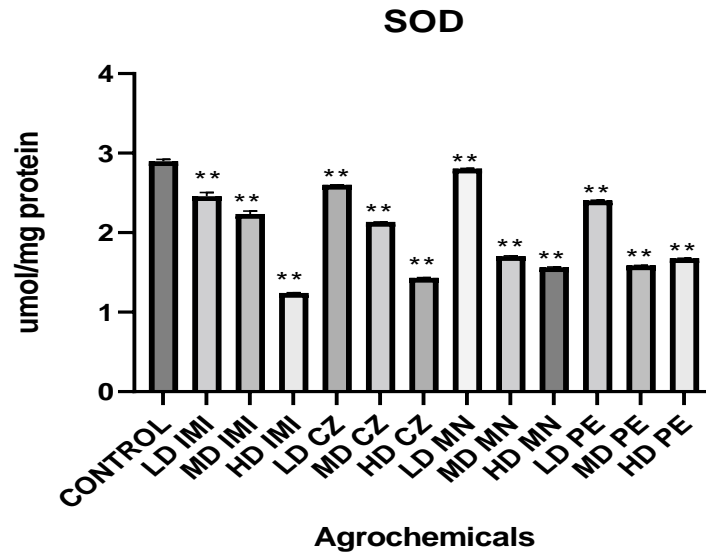


Figure 2.5 SOD level after treatment of agrochemicals. Each value represents the mean \pm SEM. (n=3), Significant level indicated by * $p < 0.05$; ** $p < 0.01$

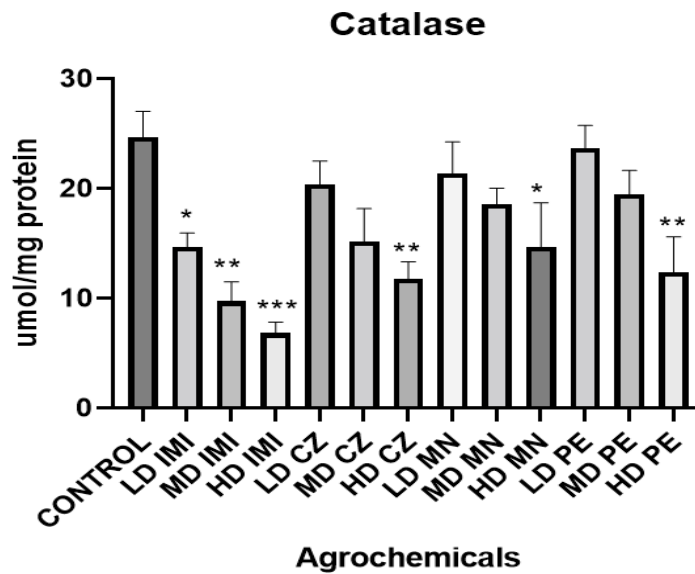


Figure 2.6 Catalase activities after treatment of agrochemicals. Each value represents the mean \pm SEM. (n=3), Significant level indicated by * $p < 0.05$; ** $p < 0.01$, *** $p < 0.001$

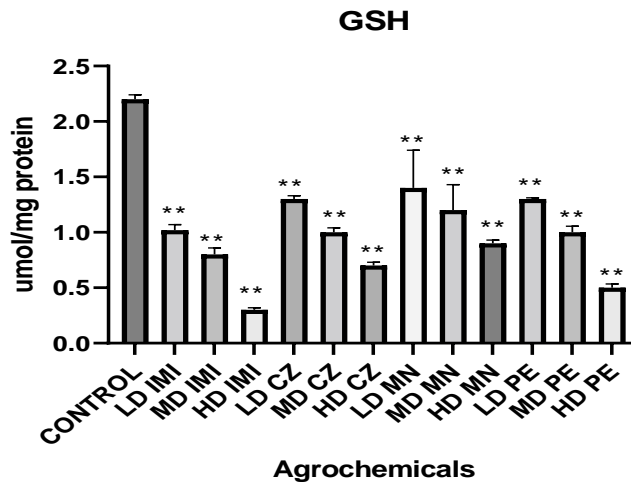


Figure 2.7 GSH level after treatment of agrochemicals. Each value represents the mean \pm SEM. (n=3), Significant level indicated by * $p < 0.05$; ** $p < 0.01$

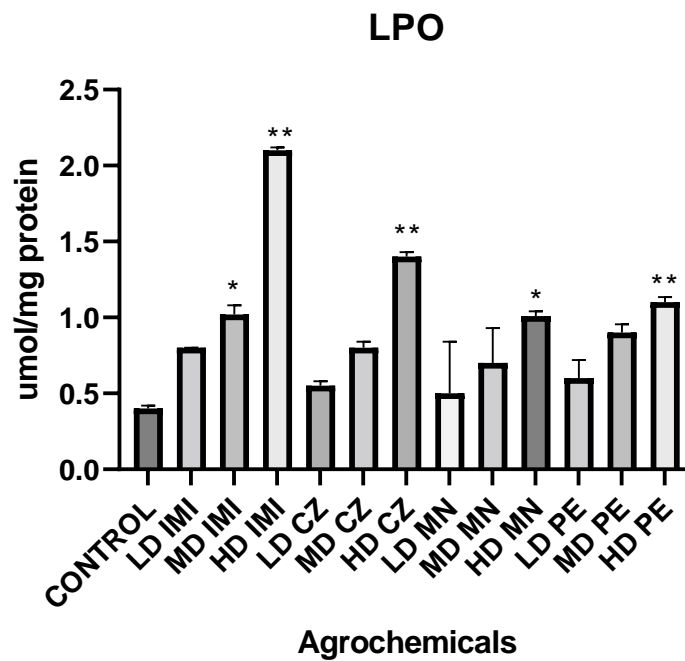


Figure 2.8 LPO level after treatment of agrochemicals. Each value represents the mean \pm SEM. (n=3), Significant level indicated by * $p < 0.05$; ** $p < 0.01$

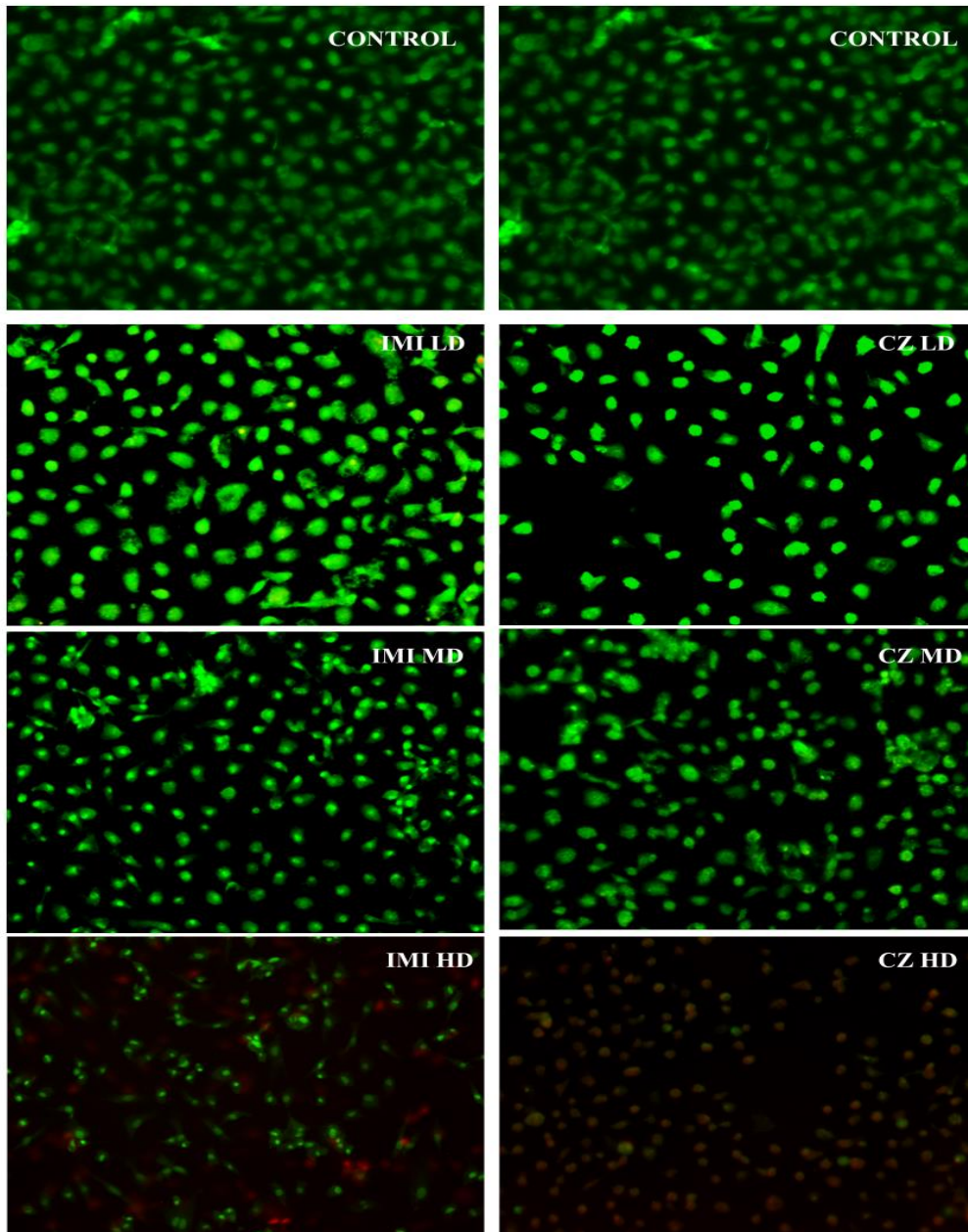


Figure 2.9 Results of Acridine orange/Ethidium bromide assay for ICG cells after 7days of treatment with sub-lethal concentrations of all agrochemicals (IMI and CZ)

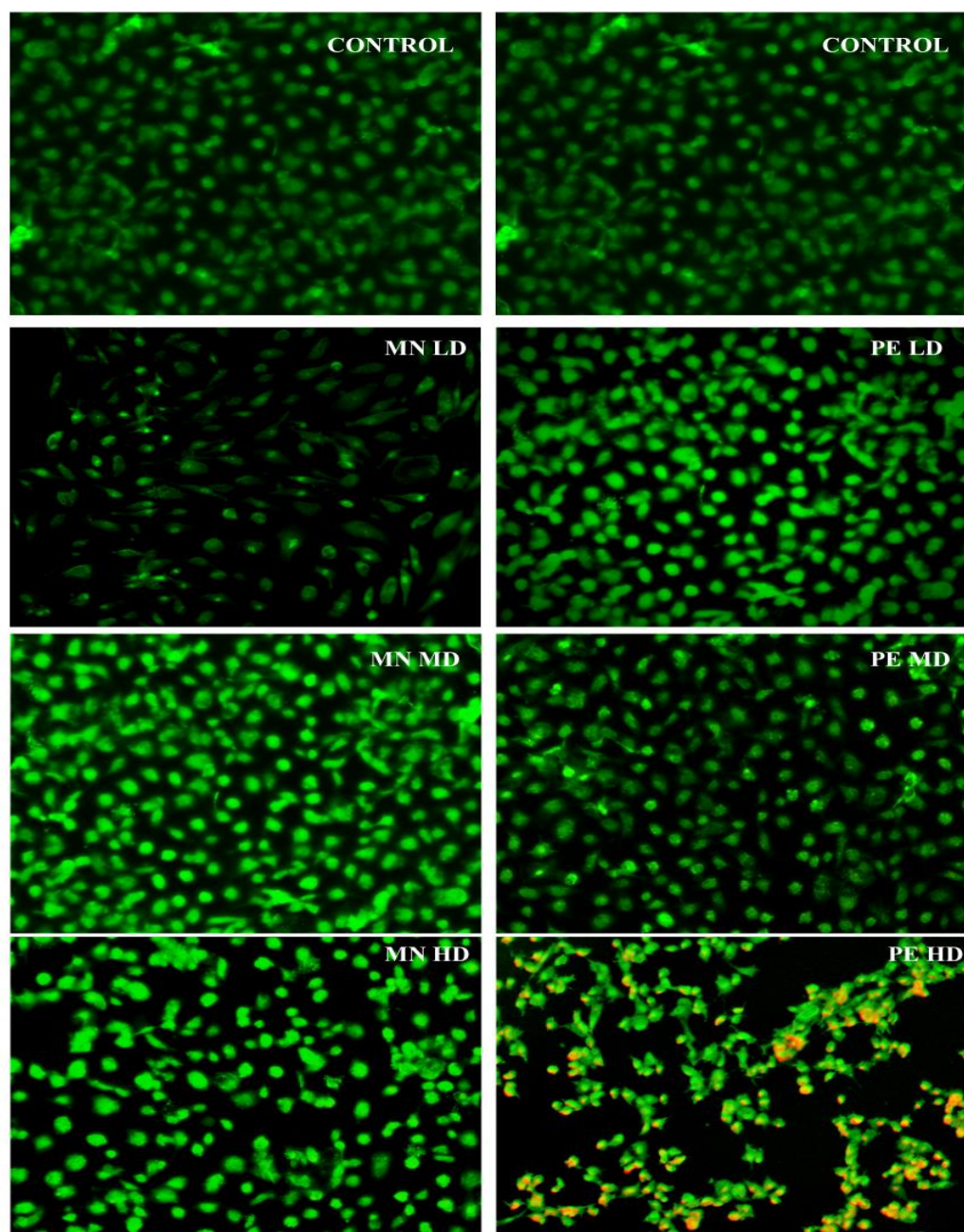


Figure 2.10 Results of Acridine orange/Ethidium bromide assay for ICG cells after 7 days of treatment with sub-lethal concentrations of all agrochemicals (MN and PE)

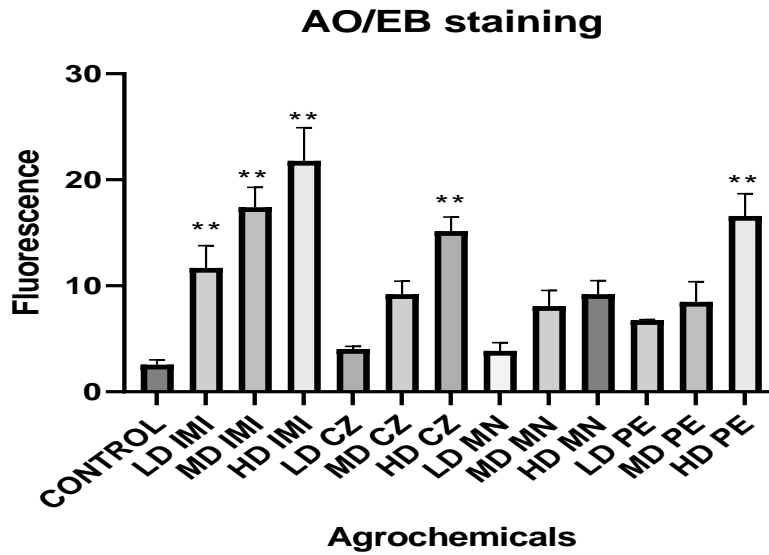


Figure 2.11 depicts result of AO/EB staining in ICG cells exposed to AGs. Each value represents the mean ± SEM. (n=3), Significant level indicated by * $p < 0.05$; ** $p < 0.01$

Agrochemicals		Fluorescence
Control		2.5661 ± 0.45
IMI	LD	11.684 ± 2.1**
	MD	17.418 ± 1.87**
	HD	21.799 ± 3.12**
CZ	LD	4.033 ± 0.25 ^{ns}
	MD	9.209 ± 1.24 ^{ns}
	HD	15.157 ± 1.34**
MN	LD	3.864 ± 0.78 ^{ns}
	MD	8.08 ± 1.47 ^{ns}
	HD	9.208 ± 1.27 ^{ns}
PE	LD	6.75 ± 0.07 ^{ns}
	MD	8.481 ± 1.9 ^{ns}
	HD	16.578 ± 2.1**

Table 2.8 AO/EB fluorescence in ICG cells exposed to agrochemicals. Each value represents the mean ± SEM. (n=3), Significant level indicated by * $p < 0.05$; ** $p < 0.01$

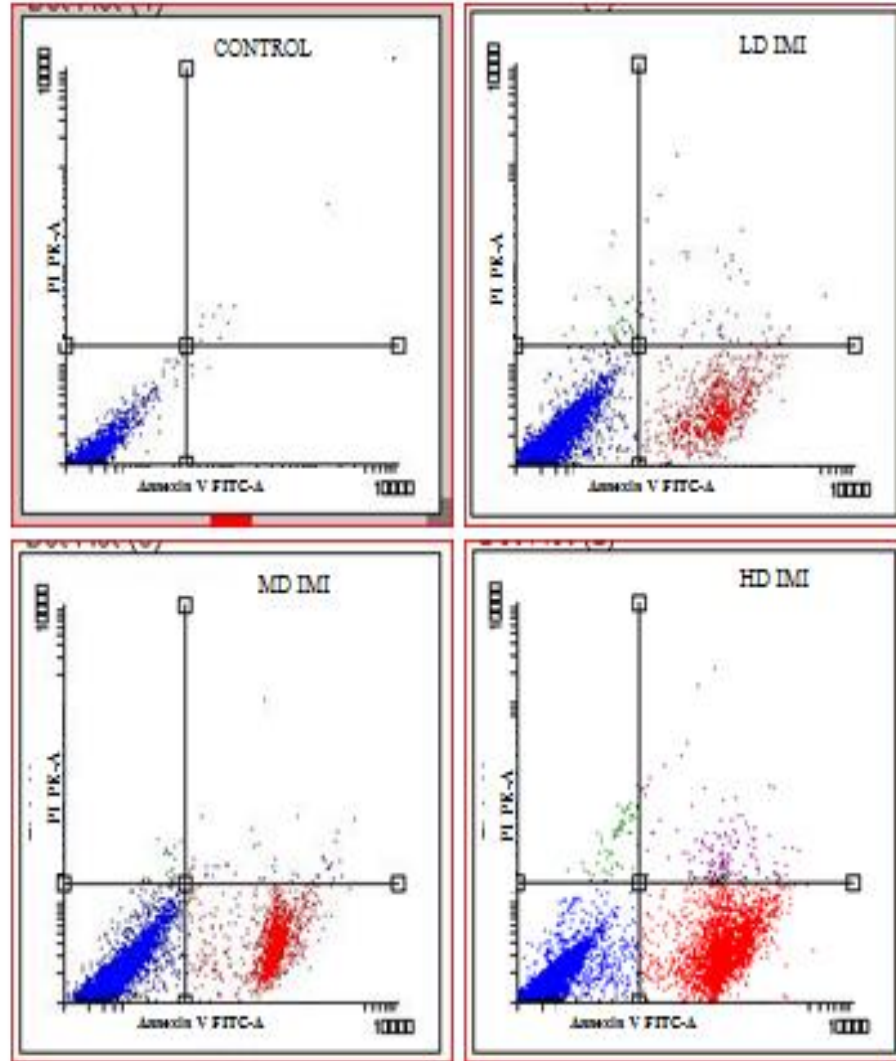


Figure 2.12 :Flow cytometry dot plots with double Annexin V-FITC/PI staining for Apoptosis of ICG cells exposed to IMI presenting Live cell (blue), Early apoptotic cells (red), Late Apoptotic cells (purple), Necrotic cells (green),

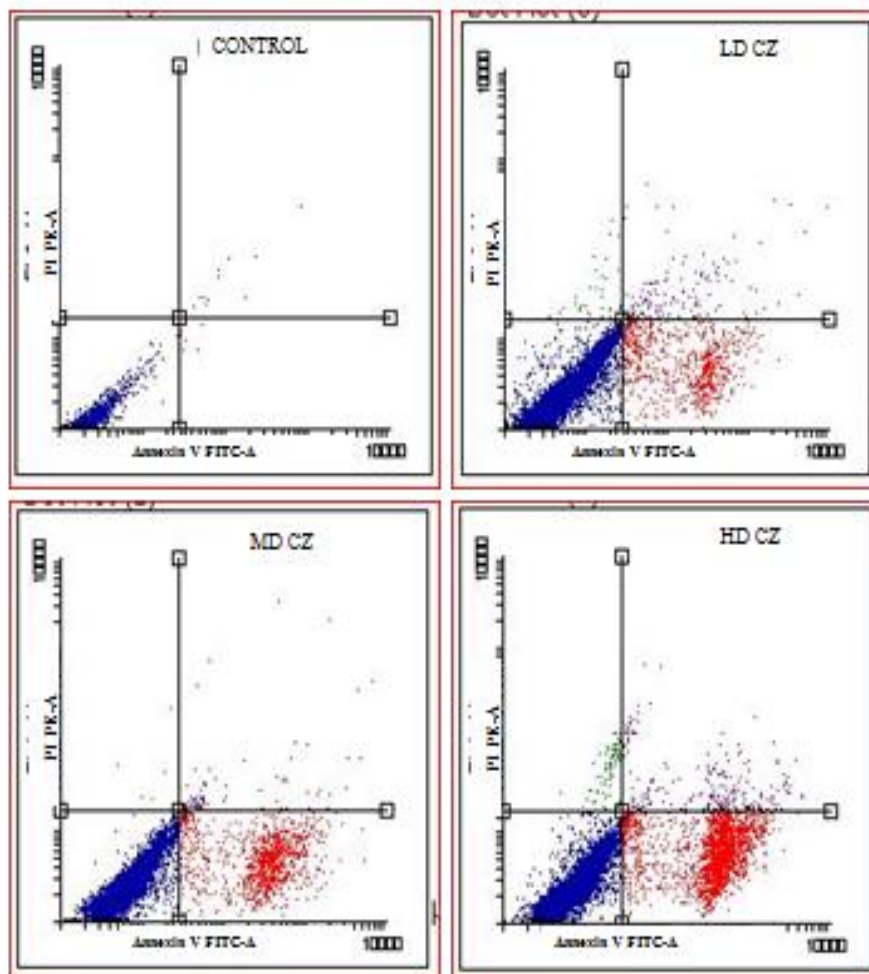


Figure2.13: Flow cytometry dot plots with double Annexin V-FITC/PI staining for Apoptosis of ICG cells exposed to CZ presenting Live cell (blue), Early apoptotic cells (red), Late Apoptotic cells (purple), Necrotic cells (green),

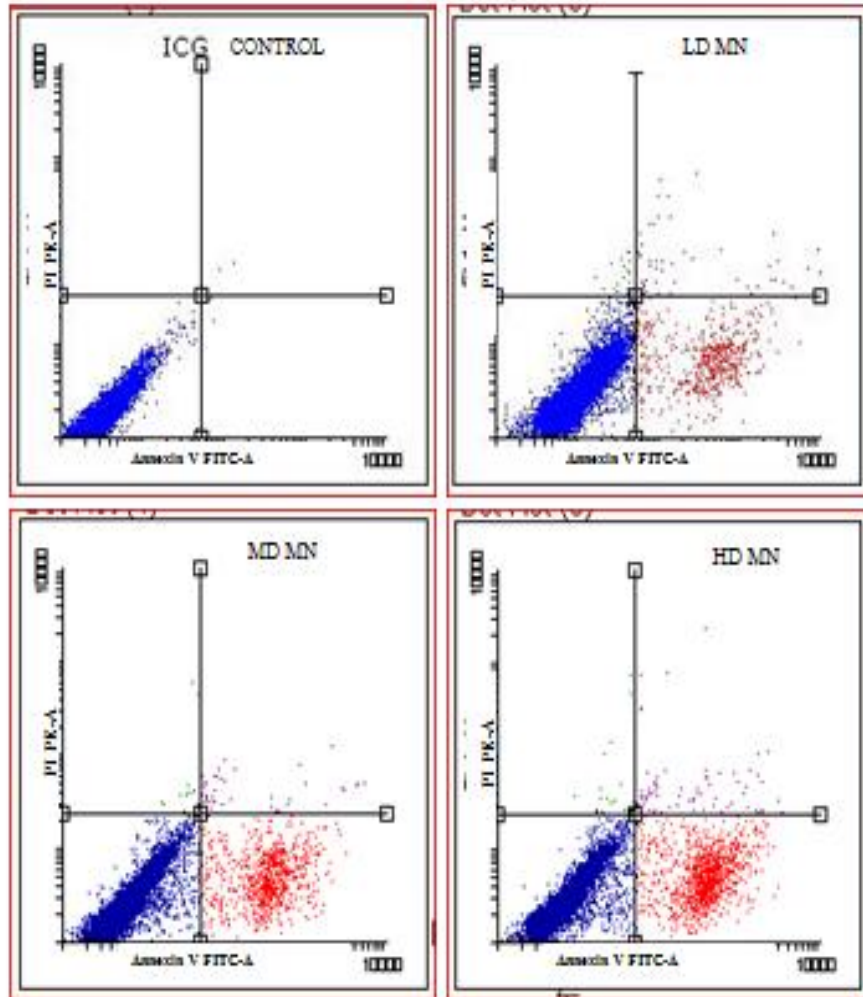
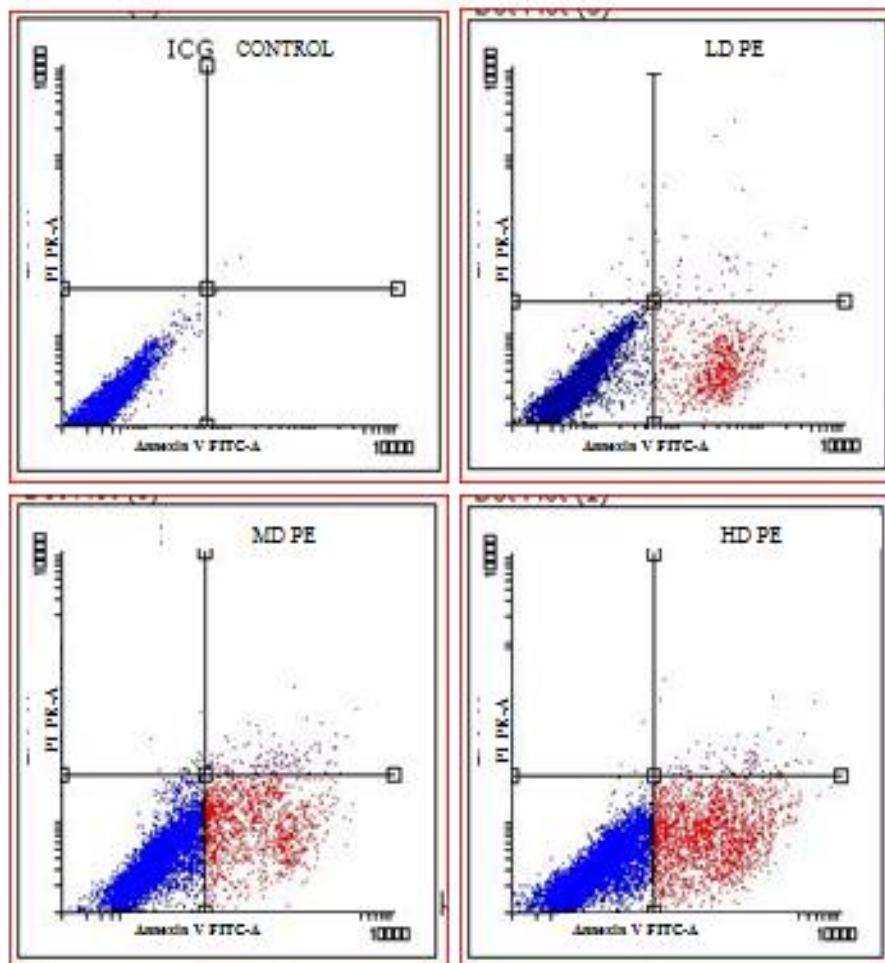


Figure: 2.14 Flow cytometry dot plots with double Annexin V-FITC/PI staining for Apoptosis of ICG cells exposed to MN presenting Live cell (blue), Early apoptotic cells (red), Late Apoptotic cells (purple), Necrotic cells (green)



2.15: Flow cytometry dot plots with double Annexin V-FITC/PI staining for Apoptosis of ICG cells exposed to PE presenting Live cell (blue), Early apoptotic cells (red), Late Apoptotic cells (purple), Necrotic cells (green)

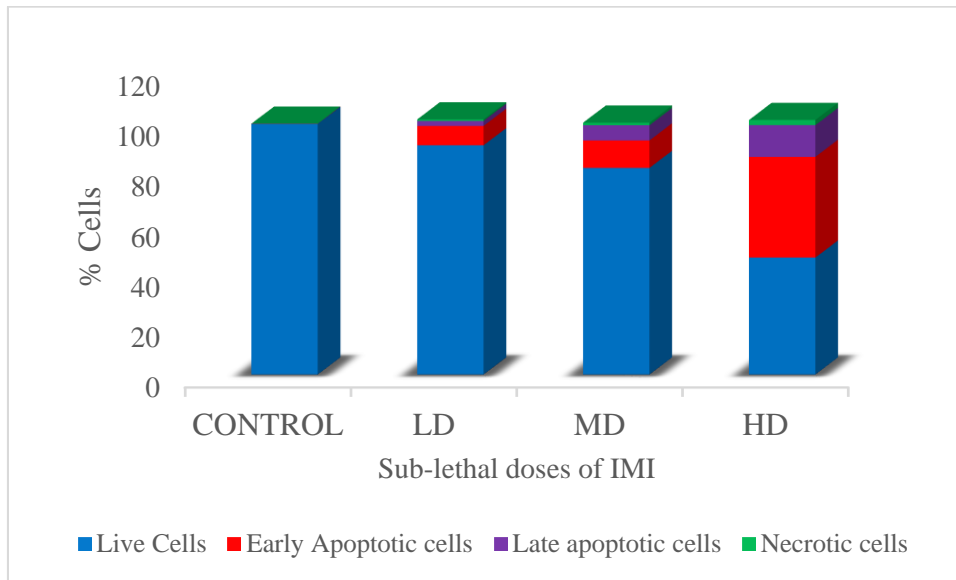


Figure 2.16: Depicts the summary data of FACS analysis of apoptosis where ICG cells were treated with sub lethal doses of IMI

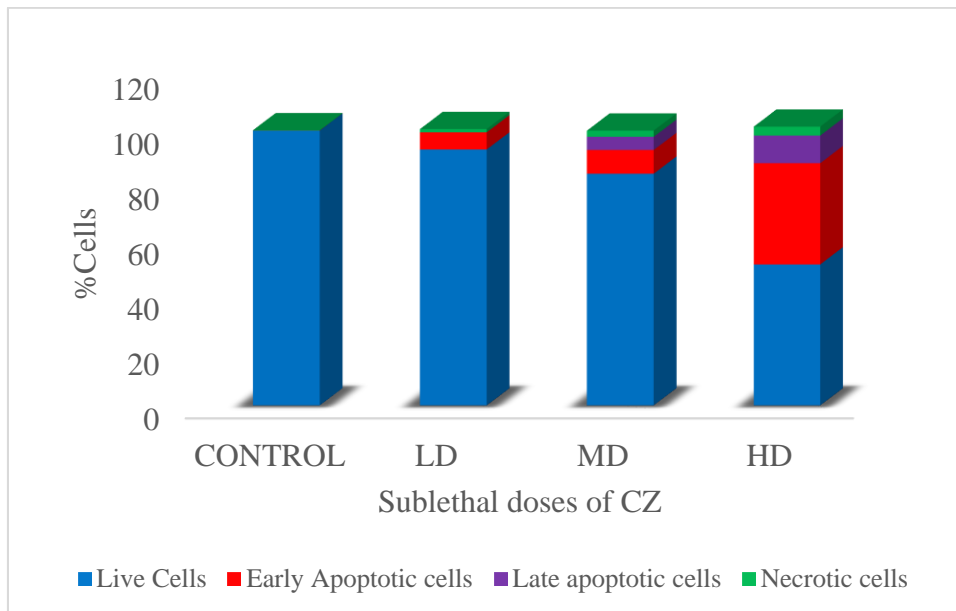


Figure 2. 17: Depicts the summary data of FACS analysis of apoptosis where ICG cells were treated with sub lethal doses of CZ

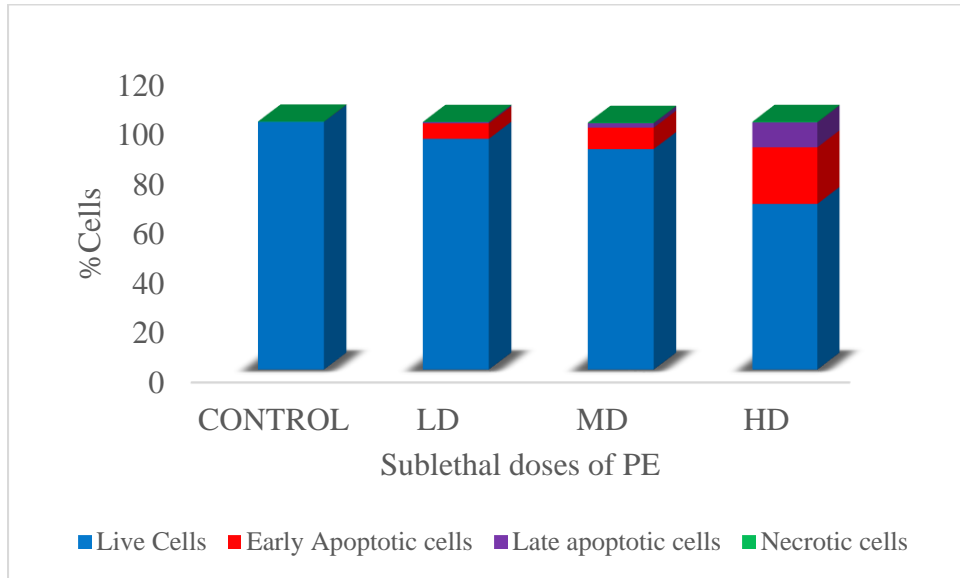


Figure 2. 18: Depicts the summary data of FACS analysis of apoptosis where ICG cells were treated with sub lethal doses of PE

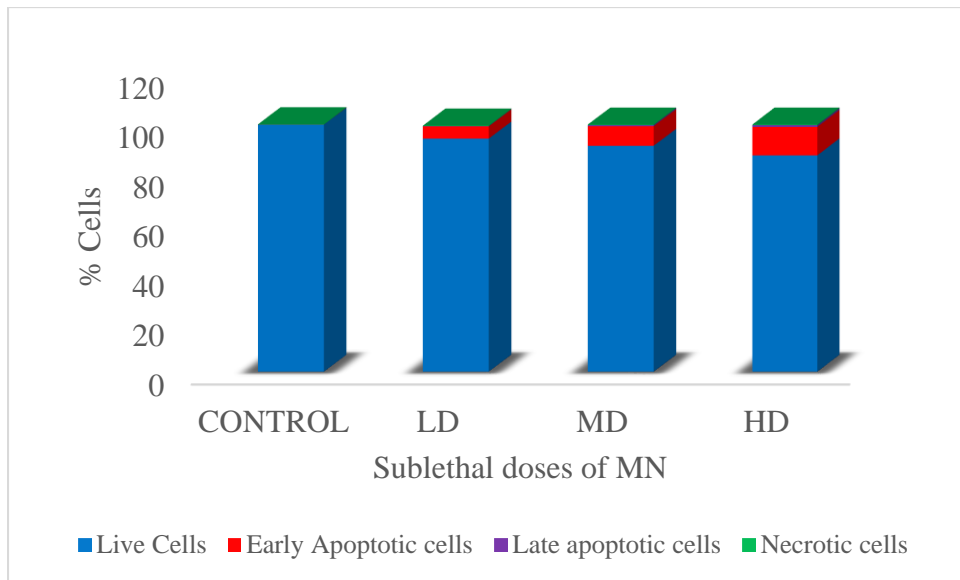


Figure 2. 19: Depicts the summary data of FACS analysis of apoptosis where ICG cells were treated with sub lethal doses of MN

AGs	Sub-lethal Dose	Live cells	Early apoptotic cells	Apoptotic cells
IMI	Control	100%	0.10%	0%
	LD	58.20%	38.10%	3.70%
	MD	41%	35%	24%
	HD	30.50%	27.40%	40.70%
CZ	Control	100%	0%	0%
	LD	75.70%	22%	2.30%
	MD	52.30%	29.20%	18.50%
	HD	47.50%	36.30%	16.2%
PE	Control	100%	0%	0%
	LD	86.30%	12.60%	1.10%
	MD	76.10%	22.60%	1.30%
	HD	62.60%	34.70%	2.70%
MN	Control	100%	0%	0%
	LD	79.50%	19.20%	1.30%
	MD	58.40%	37.3 %	4.30%
	HD	55.7 %	37.10%	7.20%

Table 2.9: Depicts the percentage status of live and dead cells of ICG cells to sub-lethal dose of AGs Each value represents the mean \pm SEM. (n=3)

Samples	concentration ng/ μ L	A ₂₆₀ /A ₂₈₀
Control	447.17	2.04
IMI LD	264.26	2.03
IMI MD	361.02	1.96
IMI HD	129.23	2.04
CZ LD	367.37	2.01
CZ MD	231.42	2.04
CZ HD	149.67	1.91
MN LD	293.85	1.89
MN MD	234.43	1.91
MN HD	267.23	1.99
PE LD	330.43	2.01
PE MD	347.21	1.89
PE HD	179.26	2.01

Table 2.10 Depicts the quantified values of total RNA and A260/A280 ratio obtained by nanodrop

Sub-acute exposure of agrochemicals resulted into a differential expression of the apoptotic as well as anti-apoptotic markers. The expression of apoptotic marker genes like bax and caspase 3 was found to be significantly upregulated ($p < 0.05$). Sub-acute exposure of agrochemicals with respect to bcl2 gene was found to be significantly decreasing ($p < 0.01$) at LD, MD and HD of IMI, CZ, and PE but sub-acute exposure showed significant decrease only at HD (Figure 2.20). Expression of caspase3 expression was found to increase significantly ($p < 0.05$) at MD and HD with respect to IMI and PE and at LD it showed non-significant increase. Sub-acute exposure of CZ and MN resulted into and significant ($p < 0.05$) increase only at HD (Figure 2.21). The expression of nfkb did not show any significant alteration at LD, but at MD and HD it showed a significant ($p < 0.05$) decrease. Agrochemical PE too did not show significant alterations in the expression of nfkb at LD and MD, but a significant ($p < 0.05$) decrease was recorded at HD (Figure 2.22). On the other hand expression of bax were up regulated significantly

($p < 0.01$) at the HD of IMI, CZ, PE and MN exposure of agrochemicals (Figure 2.23). The $\text{tnf}\alpha$ significantly up regulated in HD of IMI ($p < 0.05$) and CZ ($p < 0.01$) (figure 2.24).

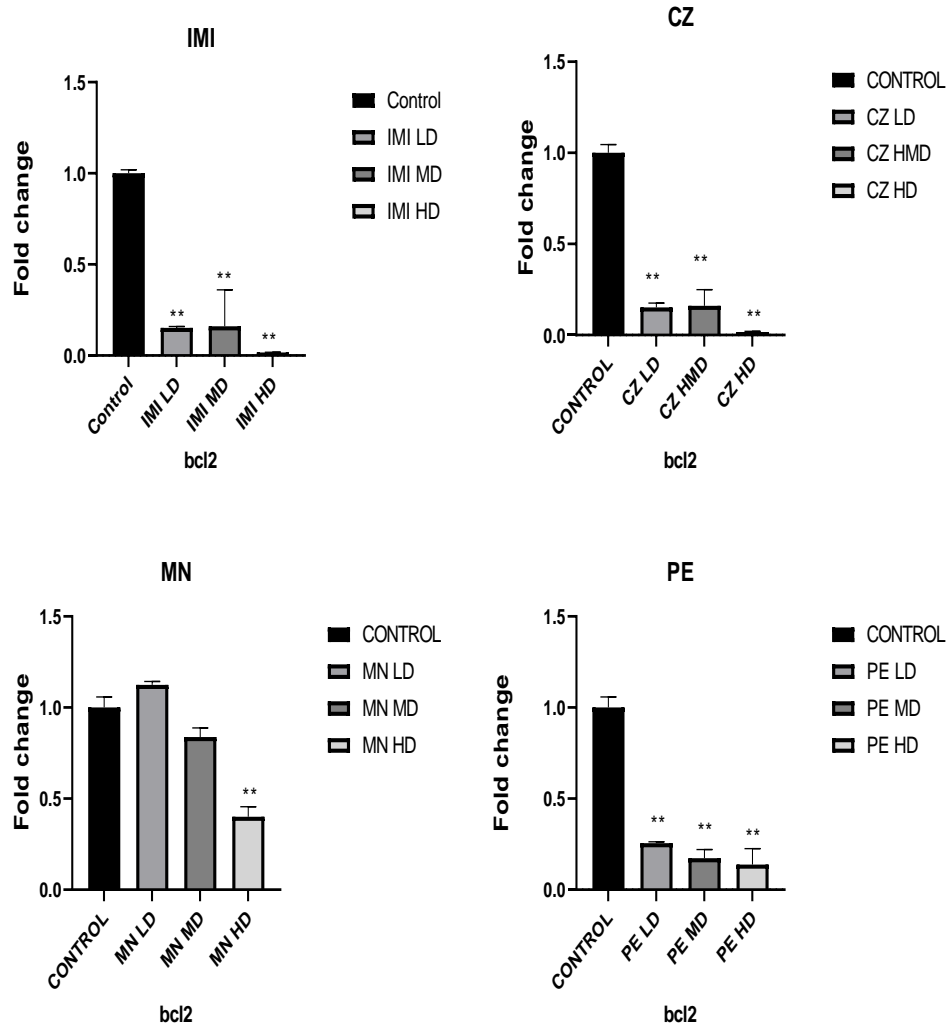


Figure 2.20 Depicts the level of bcl_2 (in folds) in ICG cells treated with sublethal doses of IMI, CZ, MN and PE. Each value represents the mean \pm SEM. ($n=3$). Significant level indicated by * $p < 0.05$; ** $p < 0.01$

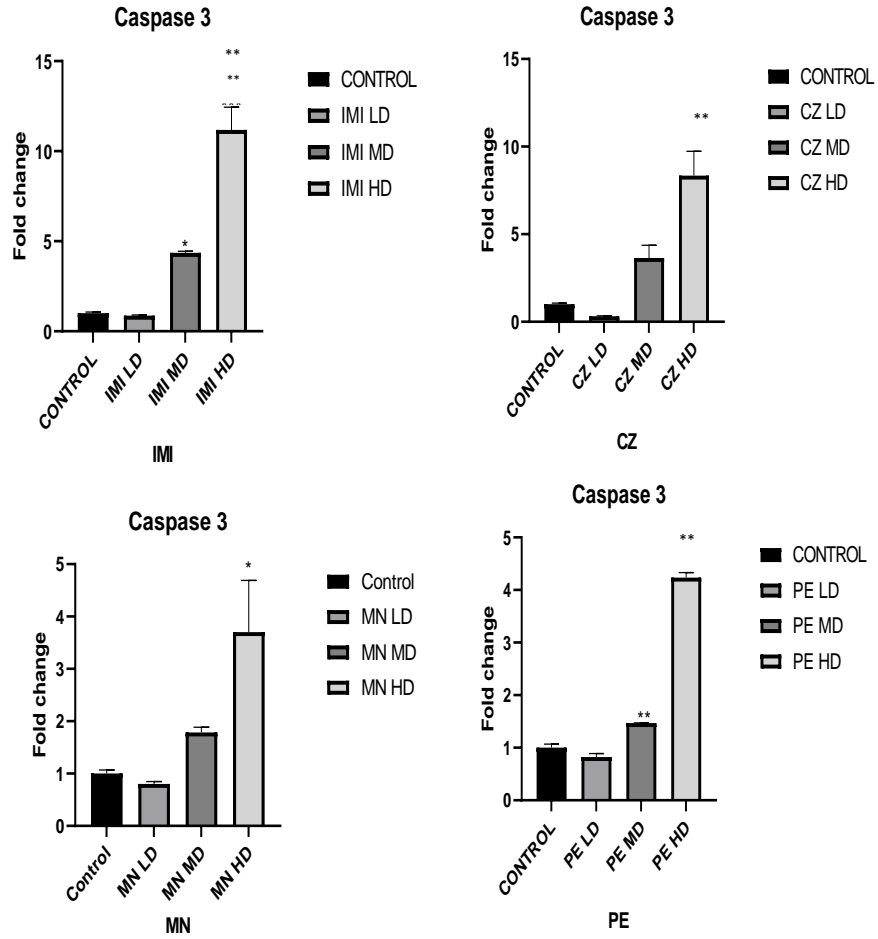


Figure 2.21: Depicts the level of caspase 3 (in folds) in ICG cells treated with sub-lethal doses of IMI, CZ, MN and PE. Each value represents the mean \pm SEM. (n=3), Significant level indicated by *p<0.05; **p<0.01; ***p<0.001.

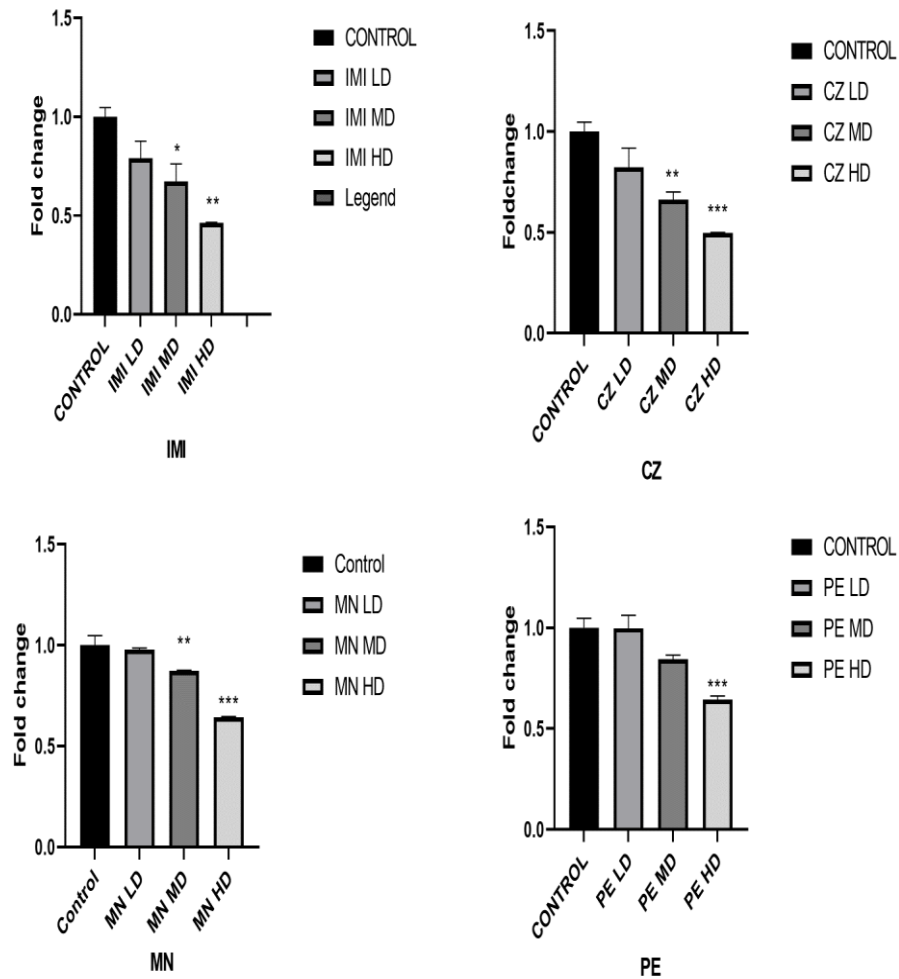


Figure 2.22 Depicts the level of nfkB (in folds) in ICG cells treated with sub-lethal doses of IMI, CZ, MN and PE. Each value represents the mean \pm SEM. (n=3), Significant level indicated by *p<0.05; **p<0.01; ***p<0.001.

**

**

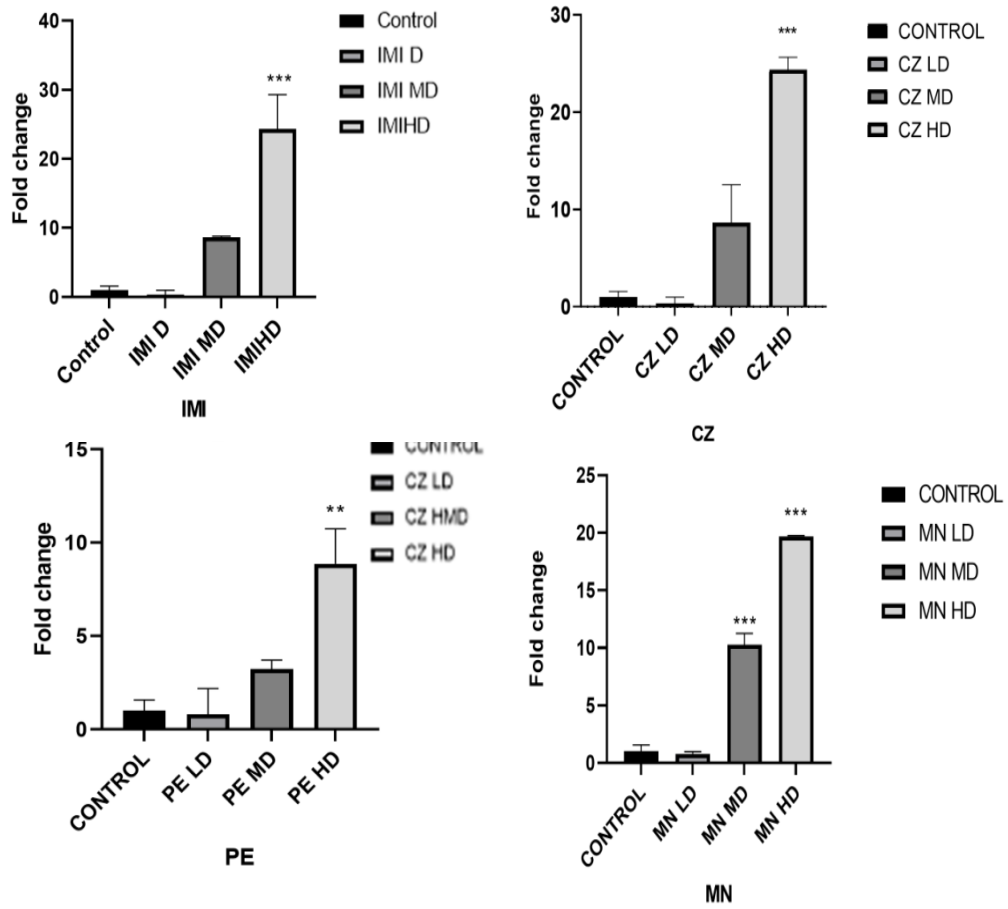


Figure 2.23: Depicts the level of Bax (in folds) in ICG cells treated with sub-lethal doses of IMI, CZ, MN and PE. Each value represents the mean \pm SEM. (n=3), Significant level indicated by *p<0.05; **p<0.01; *p<0.001.**

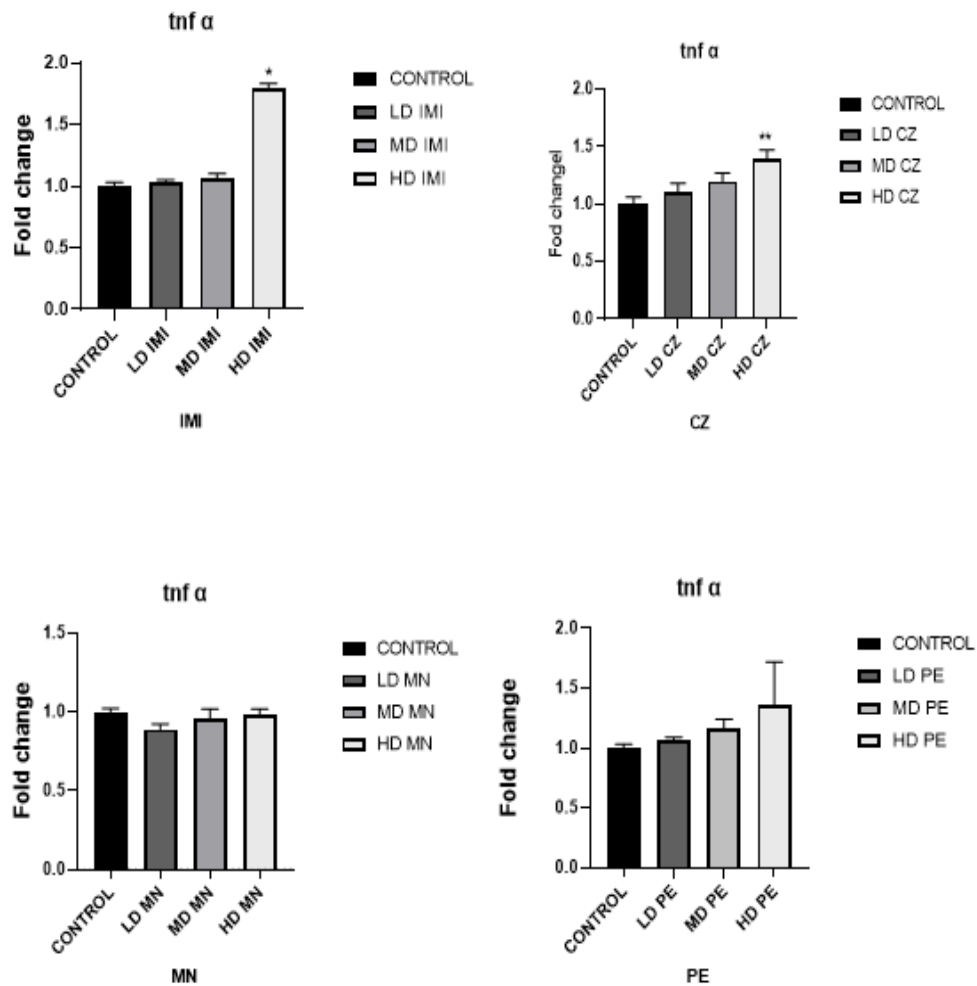


Figure 2.24: Depicts the level of *tnfα* (in folds) in ICG cells treated with sub-lethal doses of IMI, CZ, MN and PE. Each value represents the mean \pm SEM. (n=3), Significant level indicated by * $p < 0.05$; ** $p < 0.01$

AGs	bcl2	bax	cas3	nfkB	tnf α
Control	1 \pm 0.0	1 \pm 0.0	1 \pm 0.0	1 \pm 0.00	1 \pm 0.00
LD IMI	0.152 \pm 0.0123**	0.315 \pm 0.678	0.870 \pm 0.0347	0.789 \pm 0.087	1.03 \pm 0.02
MD IMI	0.160 \pm 0.346**	8.642 \pm 0.182	4.362 \pm 0.084*	0.672 \pm 0.089*	1.06 \pm 0.04
HD IMI	0.017 \pm 0.002**	24.342 \pm 4.99**	11.184 \pm 1.262**	0.463 \pm 0.002**	1.8 \pm 0.03*
LD CZ	0.1519 \pm 0.023**	0.315 \pm 0.678	0.315 \pm 0.0324	0.823 \pm 0.094	1.1 \pm 0.08
MD CZ	0.16 \pm 0.088**	8.642 \pm 3.885	3.64 \pm 0.732**	0.066 \pm 0.0367**	1.2 \pm 0.1
HD CZ	0.017 \pm 0.0029**	24.342 \pm 1.295	8.342 \pm 1.393	0.496 \pm 0.003**	1.4 \pm 0.1**
LD MN	1.12 \pm 0.0182	0.8 \pm 0.182	0.800 \pm 0.182	0.976 \pm 0.008	0.89 \pm 0.034
MD MN	0.838 \pm 0.0495	10.27 \pm 0.989**	10.273 \pm 0.989**	0.872 \pm 0.003**	0.961 \pm 0.06
HD MN	0.401 \pm 0.053**	19.70 \pm 0.038**	19.20 \pm 0.05**	0.643 \pm 0.002**	0.98 \pm 0.04
LD PE	0.256 \pm 0.0067**	0.823 \pm 1.373	0.823 \pm 1.373	0.998 \pm 0.0634	1.06 \pm 0.03
MD PE	0.173 \pm 0.0475**	3.243 \pm 0.475	3.243 \pm 0.4573	0.843 \pm 0.0216	1.17 \pm 0.07
HD PE	0.138 \pm 0.087**	8.867 \pm 1.872**	8.867 \pm 1.872**	0.643 \pm 0.017**	1.36 \pm 0.37

Table 2.11: Depicts the mean \pm SEM. (n=3) values for bcl2, bax, cas3, nfkB and tnf α . Significant level indicated by * p <0.05; ** p <0.01

2.4 Discussion

Exposure of cells to toxicants has been recognized leading to alterations in the cellular morphology characteristics. The mechanism of toxicity has been elucidated as reactive oxygen free radical attack through redox cycling. Superoxide and free radicals are formed. Such reactive oxygen species may damage many critical macromolecules, including DNA. A primary target is the cell membrane where chain-reaction lipid peroxidation is initiated, resulting in extensive membrane damage that leads eventually to loss of the functional integrity of the cell. Cells in untreated samples exhibited intact cell morphology. In contrast, treated cells exhibited a significant progressive loss of cell morphology accompanied by an increase in blebs, irregularly shaped periphery and a few apoptotic bodies. Cell sensitivity depends on a number of cell characteristics which includes chemical biotransformation and binding, membrane permeability characteristics and surface determinants, intracellular synthetic pathways and adaptive and recovery mechanisms. For some toxic chemicals, it is the functional status of the cell rather than the cell type that is critical to the function and survival of the cell. In the present study of all the exposed AGs - maximum alterations in cell morphology was observed with IMI and CZ. Our studies are in conformity of previous reports on assessment of cytotoxicity of the organophosphorus pesticide parathion on FG-9307 cells (Ilboudo et al., 2014) in RTG-2 and PLHC-1 fish cell line on exposure to sodium fluoroacetate (Zurita et al., 2007) ;in human cell lines, Hep G2 and HEK293T on exposure of benzonitrile herbicide (Lovecka et al., 2015); in the ovarian fish cell line CCO and the human cell line HeLa on exposure of imidazolium (Cvjetko et al., 2012).

Mechanism of toxicant once enters inside the cell is known to regulated by intracellular reactive oxygen species (ROS) and disorganization of the cells

(Matés et al., 2010). ROS generation damages important bio molecules and subsequently inflict deleterious effects on the organism. Highly reactive free radicals become stable by acquiring electrons from nucleic acids, lipids, proteins, carbohydrates, or any nearby molecule, causing a cascade of chain reactions resulting in cellular damage (Agarwal et al., 2008). The three major types of ROS are superoxide anion radical (O_2^-), constitutively present in cells because of leakage from the respiratory chain in mitochondria; hydrogen peroxide (H_2O_2), resulting from the dismutation of O_2^- or directly from the action of oxidase enzymes; and hydroxyl radical (OH^\cdot), a highly reactive species that modifies purine and pyrimidine bases and leading to DNA strand breaks culminating into DNA damage. ROS are produced during both normal and altered cellular function and their effects are complex and multifaceted, including beneficial effects; this dual nature of ROS means that they can also act as intracellular signaling molecules that may interfere the normal cell functioning. In the present study the dose dependent decrease in the nonenzymatic marker GSH was reported. Antioxidant scavenger, GSH which plays a role in redox buffer system is probably increasing the oxidative metabolism leading to production of electrophilic metabolites, illustrating loss of adaptive mechanism and oxidation of GSH to GSSH and thus unable to mitigate and increasing oxidative damage.

In vitro studies by Majeed et al., 2014; Nathiga Nambi et al., 2017 have reported a decrease in GSH fish cell lines on exposure to cypermethrin and chromium and in liver fish cell line PLHC-1. on exposure to Cylindrospermopsin (Gutiérrez-Praena et al., 2011) ; and in medaka (*Oryzias latipes*) cells on exposure of chromium (Goodale et al., 2008). Subsequently a significant increase in LPO was observed on exposure of the AGs, which was again found to be highest on exposure to IMI suggestive of the failure of the antioxidant defense preventing the formation of excessive free radicals (Abdel-Halim & Osman,

2020). A dose dependent increase in ROS production was observed which may be due to higher surface reactivity of this toxicant or due to its increased solubility. The increased production of ROS oxidizes cellular macromolecules causing increase in lipid peroxidation and protein oxidation in a dose dependent manner. The results are in accordance with the data obtained from in vivo assays in Teleost fish, *O.mossambicus* and *L.rohita* (Sadekarpawar et.al., 2010; Patel, 2016) and in which an increase in lipid peroxidation has been demonstrated in liver, Kidney, muscles and gill cells following exposure to these AGs. Poly unsaturated fatty acids are of utmost importance to aquatic organism as it helps in maintaining membrane fluidity at lower temperature (Monserrat et al., 2007; ; Dubey et al., 2015). These PUFAs are more prone to oxidation and thus higher degree of peroxidation is observed in aquatic organisms as compared to mammalian cells. Protein oxidation in form of protein carbonyl contents are produced in two ways. Oxidation of protein predominantly occurs via oxidation and secondarily via oxidized macromolecules produced by ROS which could be a possible explanation of high protein damage observed in the ICG cells exposed to AGs.

Level of non-enzymatic antioxidant GSH and activity of antioxidant enzyme SOD and catalase have always been considered as important biomarkers to study antioxidant defense system in animals. Dose dependent depletion of GSH and decrease in activity of antioxidant enzymes has been observed in the present study. Severe oxidative stress causes a decrease in the level of these antioxidant enzymes and hence in total antioxidant potential. The overall decrease in SOD and catalase thus is suggestive of the failure of the defence system against the oxidative stress of the AGs and the generated ROS is perhaps promoting apoptosis (Abdel-Halim & Osman, 2020). Our results are in agreement of the work of Oruc & Usta, (2007) who have reported a dose dependent decrease in the

catalase activity on exposure of Diazinon in in the muscle of *C. carpio*, further, both SOD and catalase levels have also been reported to decrease in plasma of fish and the authors have suggested the O₂ radicals or their transformation to H₂O₂ may cause oxidation of cysteine in the enzyme which results in decrease of SOD activity, and excess production of ROS may also inhibit the SOD activity (Manduzio et al., 2004; Min & Kang, 2008) As proposed by Ruas et al., (2008) the inhibition of catalase activity may be due to binding of toxicants –SH groups of enzymes, increased H₂O₂ and/or superoxide radical Thus we can conclude that the significant decrease in catalase and SOD activity in ICG cell line might have resulted from its inactivation by the superoxide radical triggered by AGs exposure (Vutukuru et al., 2006).

Apoptosis is a type of regulated programmed cell death that controls the development by eliminating physiologically redundant, physical damaged and abnormal cells. Dual acridine orange/ethidium bromide (AO/EB) fluorescent staining, visualized under a fluorescent microscope, is used to identify apoptosis-associated changes of cell membranes during the process of apoptosis. This method can also accurately distinguish cells in different stages of apoptosis. The results of enzymatic and non-enzymatic antioxidative parameters clearly revealed the failure of the defence mechanism system of the ICG cells. Hence, it was thought to confirm whether the cells are undergoing apoptosis or not. So using acridine orange/ethidium bromide (AO/EB) fluorescent staining the status of ICG cells on exposure of AGs was checked. The morphological changes on the apoptotic cell surfaces indicates that whatever apoptosis induction may be initiated, once the apoptosis begins, the cells starts to follow similar morphological changes (Kroemer & Reed, 2000). The cells were seen floating in the culture medium, were found to lose their adhering property and most of the cells were seen to get detached from the culture plates, which was an indication

that cell death has occurred. These distinctive hallmark morphological features are widely used for identification and quantification of apoptosis (Brady et.al., 2004). Apoptosis methods and protocols. Human Press, Totowa, NJ, USA). AO/EB staining on the exposure of AGs on the ICG cell line demonstrated the appearance /formation of the apoptotic bodies. Qualitative assay followed by the quantitative analyses further confirmed the toxic potential of all the AGs, where the level of toxicity was IMI>CZ>PE>MN in a dose-dependent manner compared to untreated cells. Morphological changes, like cell shrinkage, nuclear condensation, cytoplasmic disintegration as well as an increase of cell granularity was clearly observed.

Further, the cells undergoing apoptosis also exhibited loss of cell shape. Of all the AGs used, IMI and CZ unveiled relatively greater cytotoxic impacts as compared to PE and MN which clearly signifies that IMI and CZ to be more toxic than the PE and MN. After AGs exposure, oxidative stress levels and inflammation in ICG cells increased, and the mRNA and protein expression of apoptosis-related markers (bcl, bax, caspase) increased significantly, leading to apoptosis. Moreover, AO/EB staining, and flow cytometry also showed that the level of apoptotic cells increased after exposure of AGs. Our results are in accord with the work of Cui et al., (2021) who has reported Dibutyl Phthalate induced apoptosis through oxidative stress and inflammation in grass carp hepatocytes as well as work of Taju et al., (2014) who have also proved the cytotoxicity, genotoxicity and oxidative stress of malachite green on the kidney and gill cell lines of freshwater air breathing fish *Channa striata*. Cui et al., (2021) has also opined that triggers apoptosis.

Thus after confirming the qualitative status of apoptosis by AO/EB double staining, it was thought worthwhile to have a quantitative status for apoptosis by

FACS., and the analysis revealed a significantly elevated rate of apoptosis in dose-dependent manner. The outcome of the calculated FACs analysis revealed that most of the cells were in the early and late apoptosis, Of all the AGs exposed to ICG cells, maximum alterations were observed with IMI and CZ, Putting together the qualitative and quantitative observation it can thus be concluded that exposure of AGs has resulted into the generation of ROS and furthermore, the cells have undergone apoptosis.

Apoptosis is a type of genetically regulated programmed cell death that controls the development of multicellular organisms and tissues by eliminating physiologically redundant, physical damaged, and abnormal cells (Danial & Korsmeyer, 2004). Studies focusing on the genes and signals regulating apoptosis have played an important role to determine the cell death pathway (Y. Liu & Levine, 2015). Cells undergoing apoptosis activates numerous proteins in a temporally as well as spatially tightly regulated sequence. Initiation is induced by various stimuli, including the binding of ligands to cell surface receptors of the tumor necrosis factor family, damage of DNA integrity by various stress factors like toxicants or major changes of the homeostasis of cells. A main theme in transduction of many of these signals further downstreams the oligomerization and interaction of proteins with death effector domains. These proteins with conserved structural modules like death and death effector domains have a number of different functions in the cell, including connecting membrane-bound receptors to cytosolic effector caspases (Fábio et al., 2021)

Intracellular stress induces apoptosis through the intrinsic cell death pathway, while extrinsic apoptosis is initiated through transmembrane death receptors. Initiation and execution of these processes are regulated by the BCL-2 and caspase families of proteins (Danial & Korsmeyer, 2004; Galluzzi et al., 2012). Activation of the BCL-2 family members Bax and Bak results in mitochondrial outer membrane permeabilization and the release of pro-apoptotic

proteins, including cytochrome c, from the inter-membrane space into the cytosol (Eskes et al., 2000; Wei et al., 2012). Bax is a member of bcl₂ family that forms heterodimer with BCL₂ and functions as an apoptotic activator. It interacts and open mitochondrial voltage dependent anion channel (VDAC) and leads to loss in membrane potential leads to release of cytochrome c (Kratz et al., 2006). Cytochrome c can then bind Apaf-1 forming the apoptosome and activating caspase-9. Once active, caspase-9 can directly cleave and activate caspase-3. Caspase 3 interacts with caspase-8 and caspase-9 and is encoded by the cas3 gene. It is a member of the cysteine-aspartic acid protease (caspase) family.

Sequential activation of caspases plays a central role in the execution-phase of cell apoptosis. Caspases exist as inactive proenzymes that undergo proteolytic processing at conserved aspartic residues to produce two subunits, large and small, that dimerize to form the active enzyme. Caspase 3 is widely used as apoptotic marker to detect apoptosis in progress (Yabu et al., 2001). Bcl-2 which is localized at the outer membrane of mitochondria, where it plays an important role in promoting cellular survival and inhibiting the actions of pro-apoptotic proteins. The pro-apoptotic proteins in the BCL-2 family, including Bax and Bak, normally act on the mitochondrial membrane to promote permeabilization and release of cytochrome C and ROS, that are important signals in the apoptosis cascade. These pro-apoptotic proteins are in turn activated by BH3-only proteins, and are inhibited by the function of BCL-2 (Kratz et al., 2006).

In the present study the alterations in the pro-apoptotic bax which was found to be significantly increased and anti-apoptotic bcl2 genes which was found to be significantly decreased confirms their sequestration role in the intrinsic pathway of apoptosis leading to release of Cytochrome C. In the present study we have obtained a dose dependent increase in caspase 3 expression which was

significant ($p < 0.05$) at MD and HD of IMI, while for CZ, MN and PE it was only found at HD. However, the results were not same with reference to expression of bax, and the alterations were observed only at high dose for all the agrochemicals, suggesting that the elevated caspase-3 and bax activates death protease, catalyzing the specific cleavage of many key cellular proteins associated with the dismantling of the cell and the formation of apoptotic bodies which leads to program cell death (He et al., 2018). A significant dose dependent decrease in the bcl2 expression was observed for IMI, CZ and PE, while for MN it was only found at HD. BAX/BAK oligomerization is prevented by BCL2 which lead to the release of several apoptogenic molecules from the mitochondria. Decrease expression of m RNA of bcl2 suggests a decrease anti-apoptotic nature of AGs which ultimately leads to decrease in cell survival and cause cell death (Kratz et al., 2006).

NF-KB is an inducible and ubiquitously expressed transcription factor for genes involved in immune and inflammatory responses, cell survival, cell adhesion, differentiation, and growth. Given that NF-KB transcribes genes that generally control both innate and acquired immune response and play a positive effect on cell survival and proliferation. Hence, dysregulation of the mechanisms controlling its activation often can result in immune proliferative and inflammatory phenotypes (Mazzone et al., 2015). A significant decrease in the expression of NF-KB in the current studies was observed only at MD and HD of IMI, CZ and MN while for PE it was only found in HD, suggesting that the AGs impairs cell survival and that the cells have undergone program cell death. With reference to expression of $\text{tnf}\alpha$, a significant increase was observed only at HD of IMI suggesting that, CZ. PE and MN are unable to stimulation the activation of extrinsic pathway for cell death.

2. 5 Conclusion:

Overall, putting all the results it can be concluded that:

1. The exposure of all AGs in general have altered the morphology of the ICG cells
2. DCFDA staining and alterations in the enzymatic and non-enzymatic parameters have proved that AGs have induced oxidative stress.
3. AO/EB double staining along with FACS analysis and the expression of the bax, bcl2, Caspase-3, $\text{tnf}\alpha$ and $\text{nf}\kappa\text{b}$ genes confirm that the AGs are effective through intrinsic mechanistic pathway of Apoptosis.